

Title	Freezing Assisted Gene Delivery Combined with Polyampholyte Nanocarriers
Author(s)	Ahmed, Sana; Nakaji-Hirabayashi, Tadashi; Watanabe, Takayoshi; Hohsaka, Takahiro; Matsumura, Kazuaki
Citation	ACS Biomaterials Science and Engineering, 3(8): 1677-1689
Issue Date	2017-06-25
Type	Journal Article
Text version	author
URL	http://hdl.handle.net/10119/15875
Rights	Sana Ahmed, Tadashi Nakaji-Hirabayashi, Takayoshi Watanabe, Takahiro Hohsaka, Kazuaki Matsumura, ACS Biomaterials Science and Engineering, 2017, 3(8), pp.1677-1689. This document is the Accepted Manuscript version of a Published Work that appeared in final form in ACS Biomaterials Science and Engineering, copyright (c) American Chemical Society after peer review and technical editing by the publisher. To access the final edited and published work see http://dx.doi.org/10.1021/acsbmaterials.7b00176 .
Description	

Freezing Assisted Gene Delivery Combined with Polyampholyte Nanocarriers

*Sana Ahmed,^a Tadashi Nakaji-Hirabayashi,^b Takayoshi Watanabe,^a Takahiro Hohsaka^a and
Kazuaki Matsumura^{a*}*

^aSchool of Materials Science, Japan Advanced Institute of Science and Technology, Nomi,
Ishikawa 923-1292, Japan

^bGraduate School of Science and Engineering, University of Toyama, 3190 Gofuku, Toyama,
Toyama 930-8555, Japan

*Corresponding Author

E-mail address: mkazuaki@jaist.ac.jp

Tel: +81-761-51-1680

Fax: +81-761-51-1149

KEYWORDS: gene delivery, freeze concentration, polyampholytes, nanoparticles, endosomal
escape

ABSTRACT

Physical methodologies such as electroporation and the gene-gun technology have been widely used for transfection; however, their applicability is limited because they lead to cell damage and low cell viability. Therefore, to address these limitations we developed a new freeze concentration-based gene transfection system that provides enhanced *in vitro* gene delivery compared to that provided by the commercially available systems. The system employs a facile freeze concentration step, whereby cells are simply frozen to very low temperatures in the presence of polymer-pDNA complexes. As part of system development, we also synthesized a low toxicity polyethyleneimine (PEI)-based polyampholyte prepared through succinylation with butylsuccinic anhydride. In aqueous solution, this modified polyampholyte self-assembles to form small (20 nm diameter), positively charged (net surface charge of 35 mV), nanoparticles through a combination of hydrophobic and electrostatic interactions. Agarose gel electrophoresis analysis indicated that the polyampholyte nanoparticle was able to form a complex with pDNA that provided stability against nuclease degradation. Using transfection of HEK-293T cells, we demonstrated that a combination of polyampholyte: pDNA, at an appropriate ratio, and the freeze concentration method resulted in significant enhancement of GFP and luciferase expression compared to commercially available carriers. Endosomal escape of pDNA was also found to be increased when using the modified polyampholyte compared to branched PEI. This study suggests that the efficient combination of freeze concentration and the modified polyampholyte described here has great potential for *in vitro* gene therapy.

1. INTRODUCTION

Recently, gene therapy has drawn significant attention as a promising strategy for the treatment of various genetic disorders such as cancer, neurodegenerative diseases, or autoimmune diseases¹. Gene therapy requires the insertion of a gene(s) into cells in order to replace a defective gene. Usually, gene-based delivery involves encapsulation of the gene of interest in order for it to be delivered successfully to the target cells². However, nucleic acids such as DNA and RNA cannot cross the cell membrane because of both their large size and their hydrophilic nature caused by the presence of the negatively charged phosphate groups³. Generally, gene transfection is performed by one of two methods, viral (transduction), or non-viral (chemical or physical). Traditionally, gene therapy has most often been performed using recombinant viruses such as retroviruses, adenoviruses, and herpes simplex virus⁴. While the use of these vectors has been shown to be an effective method for delivering genes into cells, issues around long-term safety, including the inherent toxicity and immunogenicity of these vectors⁵, remain to be solved.

Crossing the plasma membrane is considered to be the most important and critical step in DNA transfection. In this regard, different physical methods have been designed to internalize genetic material across the cell membrane. Electroporation⁶, ultra-sonication⁷, and the use of a gene-gun⁸, are a few of the physical methods that have been reported to produce effective transfection of cells. These methods facilitate the transfer of genetic material from outside of the cell to the nucleus by creating transient membrane defects, or holes, through the use of physical force. However, these energy-based methods have severe drawbacks; for example, the high voltage required for electroporation can irreversibly damage cells and tissues and affect overall cell viability⁹. Therefore, the most challenging task in physical gene delivery methods is to design an effective method that significantly reduces the risk of cell toxicity and is easy to use.

In previous studies, we have reported the development of a freeze concentration method that can enhance delivery of proteins to cells while maintaining high cell viability^{10, 11}. Freeze concentration is a physical phenomenon that occurs during freezing at extremely low temperatures. As water crystallizes into ice crystals, the ice-crystals exclude solute molecules, thereby enhancing the concentration of the solutes around the ice crystals¹². As the temperature is lowered more and more (i.e. super-cooling), the remaining solution becomes more and more concentrated¹³. Previously, this freeze concentration technology has been effectively used in the production of fruit juices¹⁴ and for food preservation¹⁵. The freeze concentration method is also recognized as the best method for long-term preservation of the quality of the original material. We hypothesized that freeze-concentration could also be used to assist in the delivery of DNA or DNA-complexes to cells.

Although physical methods allow for effective penetration of DNA molecules into cells, the action of nucleases on the internalized naked DNA severely reduces transfection efficiency.¹⁶ Therefore, the use of non-viral carriers, prepared using chemical methods, has become an important method to provide efficient gene delivery.¹⁷ The utilization of such carriers is crucial in order to protect the gene from nuclease enzymatic degradation and thereby improve its stability¹⁸. Hence, a tremendous amount of effort has been invested in the development of new non-viral carriers that have low toxicity, but high transfection efficiency, for use in gene therapy. Improving, the transfection efficiency of non-viral carriers is a particularly difficult challenge since they generally fall far below the efficiencies of viral carriers⁴. The use of non-viral carriers that are lipid-based¹⁹, polymer-based²⁰, or are functional inorganic nanoparticles²¹, has recently expanded; in fact, some of these approaches have been used in clinical trials²⁰. Among these, polymer-based gene delivery systems have attracted a significant amount of attention for use in gene transduction.

To date, various cationic polymers including polyethyleneimine (PEI)²², poly-L-lysine (PLL)²³, chitosan²⁴ and polyamidoamine (PAMAM)²⁵ have been described as being useful as carriers for gene transfection. PLL, in particular, has been widely used as a gene delivery carrier because it protects DNA from nuclease digestion. However, despite this, PLL has the drawback that it has low transfection efficiency compared to PEI and PAMAM because of inefficient endosomal escape²⁶. Over the past few years, PEI has emerged as being the most effective gene delivery carrier and is frequently used both *in vitro* and *in vivo* with high transfection efficiency. The high transfection efficiency of PEI appears to be related to its buffering capacity. Once inside the endosome it can bind protons brought into the endosome via the endosomal ATPase. This movement of protons promotes a corresponding influx of chloride anions from the ATPase pump. Together, these ion transport events trigger endosome swelling and disruption causing the release of DNA into the cytoplasm²⁷. PEI can exist in both linear and branched forms. The linear PEI polymer lacks a primary amino group but instead contains secondary amines that link the polymer units together. On the other hand, branched PEIs contain primary, secondary, and tertiary amino groups in their polymeric backbone²⁸. However, branched PEI is also toxic towards the cells if used in excess because of strong interaction with the cell membrane that can cause cell damage²⁶.

A significant amount of effort has been made to overcome this shortcoming of PEI, primarily through modification of the primary amine in the polymeric backbone. Zintchenko et al. reported the modification of branched PEI through succinylation. This modification resulted in a modified PEI with low toxicity and efficient gene transfection capability²⁹. In another study, Yu et al. developed a non-toxic, biocompatible, modified PEI with high transfection capability after modification of PEI with amino acids³⁰. Other reports have focused on modification of PEI using PEG³¹ and sugars³².

Among other formulations, nanoparticle-based gene delivery has also gradually gained attention and they are now being extensively used as carriers. Nanoparticles have excellent physical properties including controllable adsorption and release, good particle size, and desirable surface characteristics³³.

In this study, we prepared a new self-assembled polyampholyte by modification of branched PEI (25 kDa) with a butylsuccinic anhydride (BSA). Importantly, we combined the freeze concentration methodology with this modified polyampholyte as the gene carrier and examined gene transfection efficiency. The polyampholyte we prepared was physically characterized in terms of particle size, zeta potential, and ability to bind and complex plasmid DNA (pDNA). A high transfection efficiency using the combination of freeze concentration and this modified polyampholyte was obtained, especially when compared with commercially available transfection carriers. This is the first report to explore a freeze concentration-based strategy for enhancing *in vitro* gene delivery and we expect this approach to widely improve the transfection efficiency of plasmid DNA.

2. EXPERIMENTAL PROCEDURES

2.1 Materials

Branched PEI (molecular weight 25kDa), Tris-ethylenediaminetetraacetic acid (EDTA) buffer and Dulbecco's modified Eagle's medium (DMEM) were purchased from Sigma-Aldrich (St. Louis, MO, USA), deoxyribonuclease I (DNase I, RT grade), butylsuccinic anhydride (BSA) and succinic anhydride (SA) were obtained from Wako Pure Chem. Ind. Ltd., (Osaka, Japan). The lactate dehydrogenase (LDH) cytotoxicity assay kit was purchased from Takara Bio. Inc. (Otsu, Japan). pAcGFP1-N2 plasmid was from Clontech, (Palo Alto, CA, USA),

pGL4.51[luc2/CMV/Neo] was from Promega (Madison, WI, USA) and *Escherichia coli* DH-5 α competent cells was from Takara Bio. Plus glow liquid medium was obtained from Nacalai-tesque, (Kyoto, Japan), Genopure plasmid maxi kit was purchased from Roche, (Mannheim, Germany) and ϵ -poly-L-lysine (PLL) was from JNC Corp., (Tokyo, Japan).

2.2 Transformation and purification of plasmid DNA

pAcGFP1-N2 plasmid containing the green fluorescent protein (GFP) gene and pGL4.51[luc2/CMV/Neo] containing the luciferase gene were transformed into *Escherichia coli* DH-5 α competent cells, and the transformants were streaked onto LB agar plates with the appropriate antibiotic. After incubating the plates at 37°C overnight, a colony was inoculated into Plusgrow liquid medium containing the appropriate antibiotic and cultured at 37°C, at 200 rpm overnight. The plasmids were isolated and purified from the bacterial cell culture using a Genopure plasmid maxi kit according to the manufacturer's protocol. The purified plasmids were resuspended in Tris- EDTA buffer. The concentrations of the purified plasmids were determined using a Nanodrop 1000. The plasmids were stored at -20°C until use.

2.3 Preparation of a polyampholyte cryoprotectant

To protect the components of our system from damage caused by freezing, a polyampholyte cryoprotectant was synthesized by succinylation of PLL as described in our previous reports.³⁴⁻³⁶ Briefly, an aqueous solution of 25% (w/w) PLL (10 mL) and succinic anhydride (SA) (1.3 g) were mixed at 50°C for 2 h to convert 65% of the amino groups to carboxyl groups (Scheme S1). The polyampholyte cryoprotectant is referred to as PLL-SA.

2.4 Preparation of self-assembled hydrophobically modified polyampholytes

In order to prepare the non-toxic gene carrier, we modified branched PEI by succinylation using a previously reported procedure²⁹. Briefly, PEI (0.5 g) was dissolved in 8.5 mL of water and mixed with 1.5 mL of a NaCl solution (3M). The solution was then adjusted to pH 5 using 1M hydrochloric acid. The desired amount of BSA (0.266 g, 20 mol %) was first dissolved in DMSO and was then added drop-wise to PEI to obtain BSA modified PEI (PEI-BSA). The reaction was carried out at 100°C for 2 h with constant stirring. For the preparation of succinylated PEI (PEI-SA), SA (0.171 g, 15 mol%) was dissolved in DMSO and added drop-wise to the PEI solution and reacted for 2 h at 50°C. Finally, the resultant solutions were dialyzed against water (3000 molecular weight cut off, Spectra/Por membrane) for three days. After purification, the resultant products were freeze dried. The synthesized polyampholytes were characterized by ¹H NMR. Spectra were measured in D₂O at 25°C on a Bruker AVANCE II 400 spectrometer (Bruker BioSpinInc., Fällanden, Switzerland).

2.5 Analysis of polyampholyte composition using X-Ray Photoelectron Spectroscopy (XPS)

XPS was used to analyze the composition of modified PEI derivatives. XPS excites a surface by X-ray irradiation allowing determination of the binding energy of ejected electrons. These binding energies are related to the atomic species present on the surface. To perform this, samples of the PEI derivatives (1% w/v) were prepared in PBS (-) and a small drop placed on the glass substrate. The samples were left to air dry for 4 h and then further dried under a vacuum for one day. Measurements were recorded using a VG scientific ESCALAB 250Xi spectrometer (ThermoFisher Scientific, Waltham, MA, USA) with aluminum (15 kV) as the radiation source. Photoelectrons were analyzed at a take-off angle normal to the interface. High-resolution C1s, N1s, and O1s spectra were collected with an analyzer pass energy of 20eV. The binding energy scales were referenced by setting the C1s binding energy to 285.0 eV.

2.5 Determination of the critical aggregation concentration (CAC) of the polyampholyte

The critical aggregation concentration (CAC) of the self-assembled polyampholyte was investigated using the pyrene excitation spectra method as described in our previous study¹⁰. First, 10 μL of a pyrene solution (1.0 mM in acetone) was transferred to a 10 mL glass tube. The pyrene solution was completely evaporated under a gentle stream of nitrogen. Next, the polyampholyte solution at different concentrations (10, 5, 2.5, 1.25, 0.625, 0.312, 0.125, 0.075, 0.032 and 0.01 mg/mL) was dissolved in phosphate-buffered saline without calcium and magnesium (PBS (-)) and transferred to the glass tube. Similar conditions were used for branched PEI, which served as the negative control. The resulting solutions were sonicated in an ultrasonic bath for 30 min and heated for 3 h at 65°C to equilibrate pyrene with the polyampholyte. After equilibration, the samples were left to cool overnight at room temperature. The critical aggregation concentration of PEI-BSA was estimated by examining the emission spectra of pyrene from 300 to 360 nm using a spectrofluorometer (JASCO FP-8600, Tokyo, Japan). The intensity of pyrene at 338 nm (I_{338}) and 335 nm (I_{335}) was then plotted against the concentration of polyampholyte.

2.6 Dynamic light scattering (DLS) and zeta potential

The hydrodynamic diameters of PEI-BSA and PEI-BSA/pDNA complexes were analyzed by DLS analysis using a Zetasizer 3000 (Malvern Instruments, Worcestershire, UK) with a scattering angle of 135°. The polyampholytes were dispersed in PBS (-) and the zeta potential values were measured at the following default parameters: a dielectric constant of 78.5, a refractive index of 1.6, and a concentration of 0.5 mg/mL. Data were expressed as an average of three measurements.

2.7 Agarose gel electrophoresis

2.7.1 Complex formation between polyampholytes and pDNA

A gel retardation assay was performed to confirm the pDNA condensation ability of the polymer. The gels were prepared with 1% (w/v) agarose in TAE buffer (40 mM Tris, 40 mM acetic acid, 1 mM EDTA, pH 8.5). A fixed amount of plasmid DNA (1 μ g) was then combined with different amounts of polyampholyte in 50 μ L of PBS (-). The solution was mixed gently by vortex and was incubated for 30 min at room temperature before loading onto the agarose gel. The PEI-BSA-pDNA complex and control pDNA were electrophoresed at a constant 100 V for 25 min in TAE buffer. After electrophoresis, the gel was stained with ethidium bromide and visualized using a UV transilluminator.

2.7.2 Nuclease stability test of the polyampholyte-pDNA complex

Protection of plasmid DNA from nucleases is one of the most important properties for effective and safe gene delivery both *in vitro* and *in vivo*. To examine whether the modified polyampholyte can protect the loaded plasmid DNA from nuclease digestion, we evaluated DNase I-mediated digestion of polyampholyte:pDNA complexes using agarose gel electrophoresis. Briefly, 50 μ L of PEI-BSA-DNA complexes (2:1, w/w) were incubated with different amounts of DNase I (0.1, 0.2, and 0.4 U/ μ g of DNA) in DNase I/Mg²⁺ digestion buffer (50 mM Tris-HCl, pH 7.6, and 10 mM MgCl₂). pDNA (1 μ g) was treated with DNase I at 0.1 U/ μ g as a reference. The samples were incubated in a shaking water bath (100 rpm) for 30 minutes at 37°C. Afterwards, the enzymatic digestion reaction was terminated by the addition of 5 μ L EDTA solution (0.5 M, pH 8.0) for 10 min at room temperature. To examine the release of DNA from inside the polyampholyte-DNA complex, complexes were dissociated by the addition of heparin, an anionic glycosaminoglycan, at a final concentration of 1% (w/v). The samples were further incubated in a

water bath for 3 h at 37°C. The extracted DNA samples were centrifuged and analyzed by electrophoresis on a 1 % (w/v) agarose gel in TAE buffer as described above. Undigested pDNA was used as a control.

2.8 Preparation of polyampholyte-pDNA and commercially available carrier-pDNA complexes

Briefly, the reporter genes pAcGFP1-N2 (for the GFP study) or pGL4.51 (for the luciferase study) were added to polyampholyte NPs at a fixed ratio (PEI-BSA:pDNA; w/w). The amount of polyampholyte NPs were 2, 5, 7, and 10 µg and the concentration of pDNA was fixed at 1 µg in 50 µL PBS (-). The mixture was then incubated at room temperature for 30 min. The resultant polyampholyte-pDNA complex was directly used for further study. For the control experiment, jetPEI[®] (Polyplus-transfection SA, Illkirch, France) and Lipofectamine 3000(ThermoFisher Scientific) were used as commercially available transfection carriers. These commercially available carriers have both been used extensively for gene transfection studies with great success^{21, 37}. To prepare the jetPEI[®] and pDNA complex, we followed the manufacturer's protocol. Briefly, 1 µg of pDNA and 2 µL of jetPEI[®] were dissolved in 50 µL of NaCl solution separately. Both solutions were mixed together, vortexed immediately and incubated at room temperature for at least 30 min. Similarly, to prepare Lipofectamine 3000-pDNA complexes, Lipofectamine 3000 (7.5 µL) was dissolved in opti-MEM (125 µL). Plasmid DNA (1 µg) and P 3000 reagent (5 µL) were also dissolved in opti-MEM (125 µL). The Lipofectamine 3000 and plasmid DNA solutions were gently mixed together followed by incubation at room temperature for 15 minutes to form the Lipofectamine 3000-pDNA complex.

2.9 Cell Culture

Human embryonic kidney cells (HEK-293T, American Type Culture Collection, Manassas, VA, USA) were cultured in DMEM supplemented with 10 % fetal bovine serum (FBS) at 37°C in a 5% CO₂ humidified atmosphere. When the cells reached 80% confluence, they were removed using 0.25% (w/v) trypsin containing 0.02% (w/v) EDTA in PBS (-) and were seeded onto a new tissue culture plate for subculture.

2.10 *In vitro* cytotoxicity assay

The cytotoxicity of branched PEI, PEI-SA, and PEI-BSA in HEK-293T was evaluated using the LDH cytotoxicity assay kit. Briefly, cells (1×10^3 cells/mL) were seeded into a 96 well plate with 0.1 mL of growth medium containing 10% FBS. Cells were incubated at 37°C for 72 h before the addition of test materials. Then, 0.1 mL medium containing different concentrations of polyampholytes was added to the cells, followed by incubation for 24 h. After incubation, sterile water (15 µL) was added to the samples as well as the negative control. 10 % of Triton X-100 (15 µL) was also added to each positive control well. The cultures were then incubated for 5-10 minutes at room temperature. Then, medium (90 µL) from each well was transferred to a clean 96 well-plate suitable for a plate reader. Next, LDH cytotoxicity assay reagent (10 µL) was added to each well. The samples were incubated at 37°C for 4 h in a 5% CO₂ humidified atmosphere. The resulting color intensity was measured using a microplate reader (Versamax, Molecular Devices, Sunnyvale, CA, USA) at 450 nm, and was proportional to the cell damage. Cell toxicity was quantified by normalizing against the positive control signal (i.e. HEK-293T cells incubated with 1% Triton X-100). Cell viability was investigated between the difference of total number of cells and cell damage ~~relative toxicity present~~ in each concentration of the samples. The concentration

of polyampholyte leading to 50% cell killing (IC_{50}) was calculated from a concentration-cell viability curve.

2.11 Cell freezing with polyplexes and lipoplexes

HEK-293T cells were counted and re-suspended at a density of 1×10^6 cells/mL in 10% PLL-SA cryoprotective solution. One milliliter of re-suspended cells in cryoprotectant was added to a 1.9 mL cryo-vial (Nalgene, Rochester, NY) and polymer-pDNA complexes (50 μ L, without FBS) were added and the cryo-vial was placed in a controlled freezing container providing a controlled rate of cooling of $1^\circ\text{C}/\text{min}$ in a -80°C deep freezer (Nihon freezer) and left overnight. After freezing overnight, the vials containing cells and polymer-pDNA complexes were thawed at 37°C and washed three times with DMEM medium. Cells were counted with a hemocytometer using the trypan blue staining method. Cell viability was determined as the number of viable cells divided by the total number of cells. The adsorption of non-frozen and frozen polymer-pDNA complex to the HEK-293T cells was observed using a confocal laser scanning microscope (CLSM, FV-1000-D; Olympus, Tokyo, Japan).

2.12 *In vitro* gene transfection using the freeze concentration method

After thawing, and washing three times with DMEM medium, the cells were seeded onto a glass-bottomed dish and incubated for 10 h to allow cell attachment and gene expression to occur. To create the non-frozen system for comparison, the same amount of polymer-pDNA complex was gently added to the cells and also incubated for 10 h. At the time of observation, the attached cells were washed three times with PBS (-) and GFP expression observed using CLSM.

2.13 Comparison of luciferase activity in the frozen and non-frozen systems

The transfection efficiency was evaluated by measuring luciferase activity in transfections performed using the frozen method and compared transfections performed using the non-frozen method. In this investigation, we used pGL4.51[luc2/CMV/Neo] plasmid containing luciferase reporter gene. In the case of the frozen method, the cell suspension was prepared as described above, except cells were seeded into 12 well plates. For the non-frozen method, the polymer-pDNA complex was added gently and directly to HEK-293T cells in 12 well plates. Both sets of plates were incubated for 48 h. At the time of observation, cells were washed three times with PBS (-). Cells extracts were prepared by scraping cells into lysis reagent (200 μ L/well; 25mM Tris phosphate, 2mM DTT, 2mM 1,2 diaminocyclohexane N,N,N',N' tetraacetic acid, 10% glycerol, 1% Triton X-100, pH-7.4) followed by transfer to a micro-centrifuge tube and storage on ice for 5 min prior to centrifugation at 12,000 g for 2 min. The supernatant was withdrawn and transferred to a new centrifuge tube. To measure luciferase expression, luciferase assay kit reagent (100 μ L, Promega) was added to a luminometer tube, the cell supernatant was added, the mixture vortexed, and luciferase activity was recorded using a luminometer (Berthold Technology, Lumat 3 LB 9508). The luminometer program was adjusted to perform a 2 s measurement delay followed by a 10 s measurement for luciferase activity. The luciferase activity was expressed as relative light unit (RLU) and results were normalized to total cell protein measured by using bicinchoninic acid (BCA) protein assay kit (ThermoFisher Scientific). All experiments were performed in triplicate.

2.14 Intracellular localization of DNA in HEK-293T cells

Thawed HEK-293T cells containing 10% cryoprotectant and either branched PEI: pDNA (2:1, w/w) or PEI-BSA:DNA (2:1,w/w) were seeded onto a glass-bottomed dish at a density of 1×10^3 cells/mL. The plasmid used was pAcGFP-N2 labeled with Cy3 dye. The cells were incubated

for a further 24 h in a 5% CO₂ humidified atmosphere at 37°C. LysoTracker Green® DND-26 and Hoechst dye were then added and the cells incubated for 30 min further prior to analysis. Samples were rinsed with PBS buffer and the cells were counterstained with LysoTracker Green for endosomes and cell nuclei were stained with Hoechst 33342 prior to imaging using CLSM.

2.15 Statistical analysis

All data are expressed as means ± standard deviation (SD). All experiments were conducted in triplicate. To compare data among more than three groups, a one-way analysis of variance (ANOVA) followed by the Bonferroni post-hoc test was used. A P value of <0.05 was considered statistically significant.

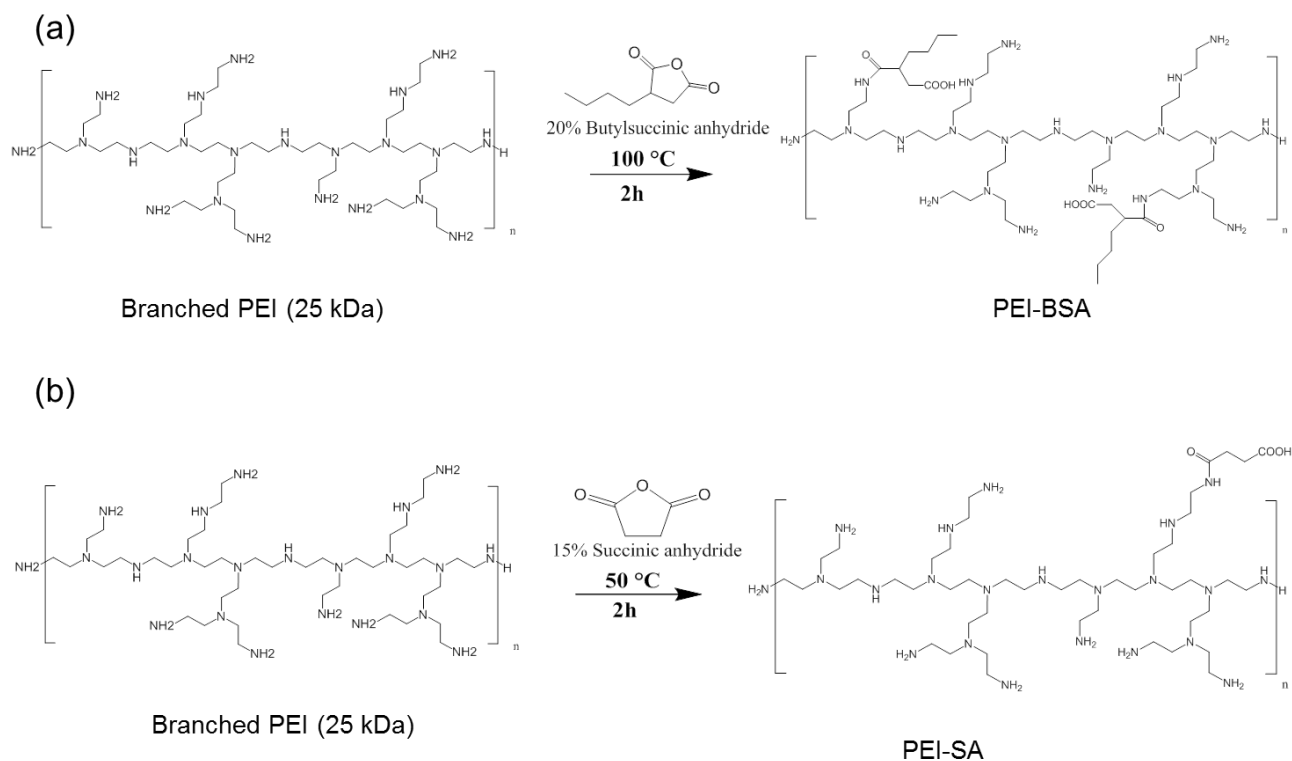
3. RESULTS AND DISCUSSION

3.1 Preparation of polyampholyte as acryoprotectant

In a previous study, we developed a new, non-toxic, polyampholyte cryoprotectant that protected cells from freezing-induced damage³⁴. This polyampholyte cryoprotectant was synthesized by succinylation of PLL with succinic anhydride (SA). Succinylation of PLL with 65 mol% of SA introduced carboxyl groups as a result of the reaction of SA with amino groups. The polyampholyte cryoprotectant is referred to as PLL-SA (Scheme S1). The synthesis of polyampholyte cryoprotectant was confirmed by ¹H-NMR in D₂O (Figure S1). From the ¹H-NMR spectra it was found that 63% of the amino groups in PLL were succinylated. This cryoprotectant has been used previously for the cryopreservation of various cell lines with low toxicity.

3.2 Preparation of self-assembling hydrophobic polyampholytes

For the preparation of the nanocarrier, we developed a new amphiphilic self-assembled hydrophobic polyampholyte by modifying branched PEI with hydrophobic BSA(20 mol%) to yield PEI-BSA. The reaction is shown in Scheme 1a. We also prepared a second polyampholyte, where branched PEI was modified with SA to yield PEI-SA, as shown in Scheme 1b. The modified PEIs were compared with PEI using ^1H NMR in D_2O (Figure S2). We observed that unmodified PEI displayed a proton signal around 2.5-3.0 ppm (Figure S2a). After succinylation with succinic anhydride, the peak separated into three different peaks at 2.5, 3.2, 3.5 ppm respectively. Peaks above 2 ppm and below 4 ppm are associated with CH_2 proton signals and so the three new peaks might be associated with the primary, secondary, and tertiary amines of branched PEI, respectively (Figure S2b). Moreover, on further substitution of branched PEI with hydrophobic BSA, we observed a new peak at 1.1 ppm, which represents the methyl group from BSA (Figure S2c). The two CH_2 proton signals at 1.6 and 1.8 ppm belong to the CH_2 signals of the butyl group (Figure S2c). Furthermore, the degree of substitution of succinic anhydride and butylsuccinic anhydride on branched PEI was measured using XPS analysis and is shown in Table 1. The substitution was calculated as a function of percent atomic oxygen content present in the polymers. From this, we calculated the degree of substitution (DS) of SA in PEI-SA to be 9.38 % and the DS of BSA in PEI-BSA to be 9.35 % (Table 1). These DS values were smaller than the feeding ratio (for PEI-SA: 15%, for PEI-BSA: 20%), suggesting steric hindrance of the substituted chain. The binding energies of each element in the samples are shown in Figure S3 and detailed analysis of the calculation of degree of substitution is shown in Table S1.



Scheme 1 (a) Preparation of a hydrophobically modified polyampholyte by modification of branched PEI using BSA (b) Preparation of a polyampholyte by modification of branched PEI using SA.

Table 1 Determination of the degree of substitution by elemental analysis (atomic (At) %) using XPS

Samples	C (At%)	N (At%)	O (At%)	Degree of substitution (%)
PEI-SA	70.552	21.780	7.692	9.38
PEI-BSA	73.228	19.861	6.909	9.35

3.2 Characterization of the polyampholytes

3.2.1 Critical aggregation concentration (CAC)

We characterized the critical aggregation of PEI-BSA and branched PEI by measuring the pyrene fluorescence excitation spectra at 25°C. Pyrene is highly hydrophobic and therefore its solubility in water is very low but it can easily solubilize into the hydrophobic region of macromolecules. The pyrene excitation spectra of PEI-BSA, at different concentrations of the polyampholyte, are shown in Figure 1a. Figure 1b shows the variation in the pyrene fluorescence intensity ratio (I_{338}/I_{335}) in relation to polymer concentration. The intensity ratio significantly increased with increasing polymer concentration; the CAC value was estimated from the cross-point on the graph and was around 0.625 mg/mL, suggesting that the association between polymer side chains via inter- or intra-molecular association leads to the formation of aggregates at concentrations above this. Further, as a negative control, we determined the critical aggregation concentration for branched PEI. As expected, the branched PEI did not show any aggregation behavior with increasing concentration (Figure S4). These data support that the polyampholytes were self-assembled due to self-aggregation occurring at a particular concentration.

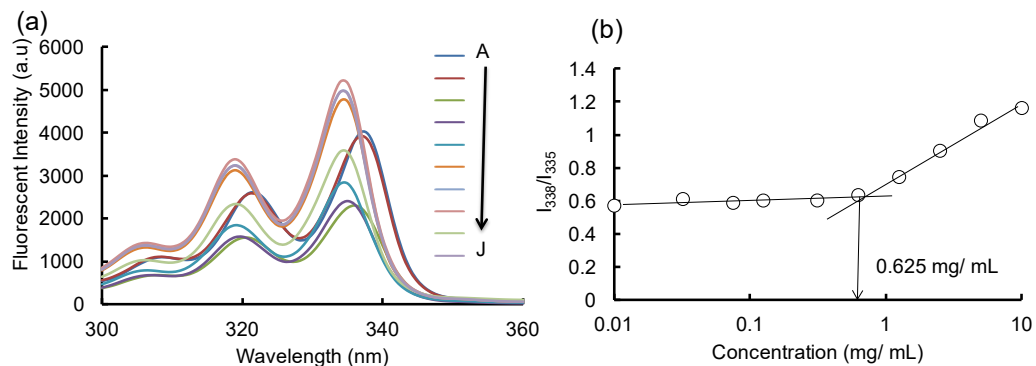


Figure 1. CACs of PEI-BSA. (a) Pyrene excitation spectra (A-J) of PEI-BSA solutions at different polyampholyte concentrations, 10, 5, 2.5, 1.25, 0.625, 0.312, 0.125, 0.075, 0.032 and 0.01 mg/mL, respectively. (b) The ratio of I_{338}/I_{335} against polyampholyte concentration.

3.2.2 Particle Size

Particle size is an important factor that can influence the internalization of particles across the plasma membrane. Therefore, we investigated the particle size of PEI-SA and PEI-BSA in PBS buffer (10 mg/mL) at physiological pH using DLS analysis. We found that the particle size of PEI-BSA was extremely small, being around 20.7 ± 0.6 nm in diameter with a narrow size distribution (polydispersity index (PDI) 0.3) (Table 2). On the other hand, PEI-SA was much larger, having a particle size around 147.9 ± 44.0 nm in diameter (Table 2). The reason for this might be related to the presence of self-aggregates in PEI-BSA, which would lead to reorganization into compact particles. These self-aggregates are likely to be formed via non-covalent attractive forces such as intermolecular hydrophobic and electrostatic interactions. Many studies have reported that nanoparticles smaller than 200 nm enter cells more efficiently and more rapidly than larger particles³⁸.

Table 2 Characterization of polyampholytes including diameter, zeta potential, polydispersity and CAC in PBS (-) buffer (10 mg/mL) at pH7.4.

Samples	Diameter ^a (nm)± SD	Zeta potential (mV) ± SD	CAC ^b (mg/mL)	PDI
Branched PEI	ND	51.9± 0.8	0.000	ND
PEI-SA	147.9± 44.0	41.8± 1.2	ND	0.62
PEI-BSA	20.7± 0.6	34.4± 3.5	0.625	0.33

^aDetermined by DLS.

^bDetermined by using excitation spectra of pyrene.

3.2.3 Surface charge

Nanoparticle properties such as positive surface charge are extremely important for an efficient interaction with the cell membrane. In our study, we found that branched PEI had a highly positive surface potential, being around 51.9±0.8mV. Following succinylation of PEI with succinic anhydride, the positive charge density of the polymer was reduced, with PEI-SA having a zeta potential of 41.8±1.2mV. Further, modification with hydrophobic butylsuccinic anhydride led to a larger decrease in surface potential to 34.4±3.5mV. The reduction in positive surface charge is likely reflective of the reduced number of amine groups in the polymeric chains after modification by BSA or SA, as shown in Table 2.

3.3 Characterization of pDNA loaded polyampholytes

3.3.1 Particle Size

We next evaluated the particle size of PEI-BSA and pDNA-loaded PEI-BSA in the presence of PBS(-) buffer at physiological pH. As expected, the particle size of the latter was drastically increased due to the strong electrostatic interactions between PEI-BSA and the pDNA, compared with PEI-BSA, as shown in Figure 2a. The particle size of PEI-BSA was 18 nm but increased to 255 nm after pDNA adsorption. For efficient gene transfer, the carrier-pDNA complex should be small and compact. The formation of a complex between PEI-BSA and pDNA with both a suitable size and surface charge is an important criterion for polycations, when used as gene carriers for internalization into cells. For this reason, we evaluated the particle size of the PEI-BSA-pDNA complex, as a function of the PEI-BSA:pDNA (w/w) ratio over a range from 0.25 to 10. The particle sizes of PEI-BSA:pDNA complexes plotted against the PEI-BSA:pDNA (w/w) ratios are shown in Figure 2b. We found that the size of the PEI-BSA-pDNA complex decreased with increasing PEI-BSA concentrations. The size of pDNA without PEI-BSA was around 1979 ± 181.5 nm as 0:1 w/w ratio of PEI-BSA:pDNA. However, when the PEI-BSA:pDNA (w/w) ratio reached 2:1 and 5:1, the particle sizes were around 280.33 ± 207.2 nm and 117.26 ± 12.4 nm respectively, as shown in Figure 2b. This reduction in size likely arises as a result of the formation of an optimized PEI-BSA-pDNA complex, which maximizes ionic interactions. From these data, it is clear that PEI-BSA can condense pDNA into a nano-sized complex that is suitable for endocytic cellular uptake.

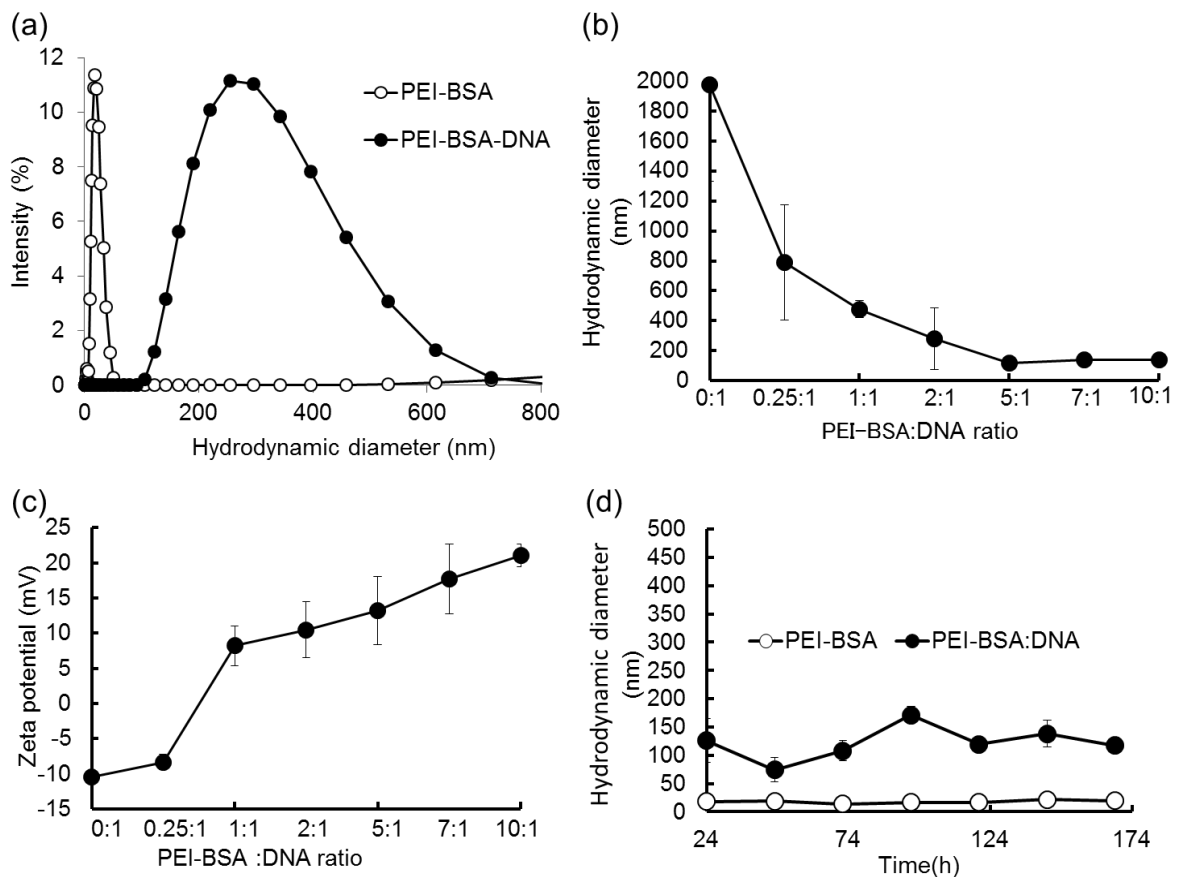


Figure 2. Physical characteristics of polyampholytes in PBS(-) buffer under physiological conditions (a) Comparison of polyampholyte particle sizes, with or without pDNA, measured by DLS analysis. Open circle, PEI-BSA alone, closed circle, PEI-BSA-pDNA. (b) Hydrodynamic diameter and (c) Zeta potential and of PEI-BSA-pDNA complexes at different PEI-BSA/pDNA ratios ranging from 0:1 to 10:1 (d) Particle size stabilities of PEI-BSA (2 μ g) without DNA and a PEI-BSA:pDNA(2:1, w/w) complex over time at 25°C.

3.3.2 Surface charge

Similarly, we also characterized the zeta potential of PEI-BSA and pDNA complex at different polyampholyte:DNA w/w ratios. As shown in Figure 2c, the surface potential of the different polyampholyte-pDNA complexes tends to become more positive as the concentration of

polyampholyte increased. The zeta potential of bare DNA without PEI-BSA was found to be at -10.48 mV when the polyampholyte:pDNA (w/w) ratio was 0:1, whereas the surface potential rapidly increased to a positive value as the polyampholyte:pDNA (w/w) ratio was increased to 1:1. Overall, we observed that the zeta potential of the PEI-BSA-pDNA complex escalated from -8.31±1.0 to 21.02±1.6 mV as the PEI-BSA:pDNA (w/w) ratio increased from 0.25:1 to 10:1. This change in positive charge of the PEI-BSA-pDNA suggests that the efficient complexation of pDNA with PEI-BSA that can be observed by measuring the surface charge potential. Based on this, it was apparent that PEI-BSA was able to condense pDNA at PEI-BSA/ pDNA ratios ranging from 1:1 to 10:1.

3.3.3 Stability

A long half-life is considered to be an essential property for nanoparticles to effectively deliver a target gene into the target cell or tissue of interest. Therefore, the inherent stability of polymer-pDNA complexes is very important in successful delivery of genetic-based materials. Consequently, in this study, we characterized the physical stability of PEI-BSA-pDNA complexes over a period of seven days under physiological conditions, both in the presence and absence of pDNA. We found that the size of un-complexed PEI-BSA did not change over this timeinterval, as shown in Figure 2d. This result suggests that the introduction of a hydrophobic modification such as butylsuccinic anhydride on branched PEI can improve the nanoparticle stability presumably due to the compact self-assembled nanostructure. Similarly, the PEI-BSA-pDNA complex also maintained a stable size over this one-week period (Figure 2d). These data strongly suggest that the stability of PEI-BSA-pDNA complexes arises because of electrostatic interaction leading to efficient compaction of the pDNA.

3.3.4 Agarose gel electrophoresis studies

3.3.4.1 Complex formation between pDNA and polyampholytes

DNA condensation is required in order for a PEI-BSA-pDNA complex to be formed. The complexation and binding ability of PEI-BSA with pDNA was measured by agarose gel electrophoresis. The PEI-BSA-pDNA complexes were prepared by varying the concentration of PEI-BSA from 0.25 to 10 μg while the concentration of pDNA was fixed at 1 μg in 50 μL PBS (-) (Figure 3a). As shown in Figure 3a, uncomplexed pDNA was clearly visible. After the introduction of PEI-BSA at a ratio of 0.25:1 (w/w) a band corresponding to un-complexed pDNA was still clearly visible. However, as the PEI-BSA: pDNA ratio increased above 0.25:1 (i.e. 1:1 to 10:1) it was apparent that the band corresponding to the un-complexed pDNA disappeared. This could be explained by the fact that once pDNA was associated with the PEI-BSA, it was too large to diffuse through the agarose gel matrix and therefore could not undergo electrophoresis. Instead of moving towards the positive electrode, it might have the possibility to move in opposite directions because of change in the surface charge of polymer-DNA complex. The results of agarose gel electrophoresis indicated that PEI-BSA may bind with pDNA at different mass ratios of polymer to pDNA to form complexes (Figure 3a). In addition, these results were clearly in good agreement with the data showing size and zeta potential of the PEI-BSA-pDNA complex (Figure 2b, c).

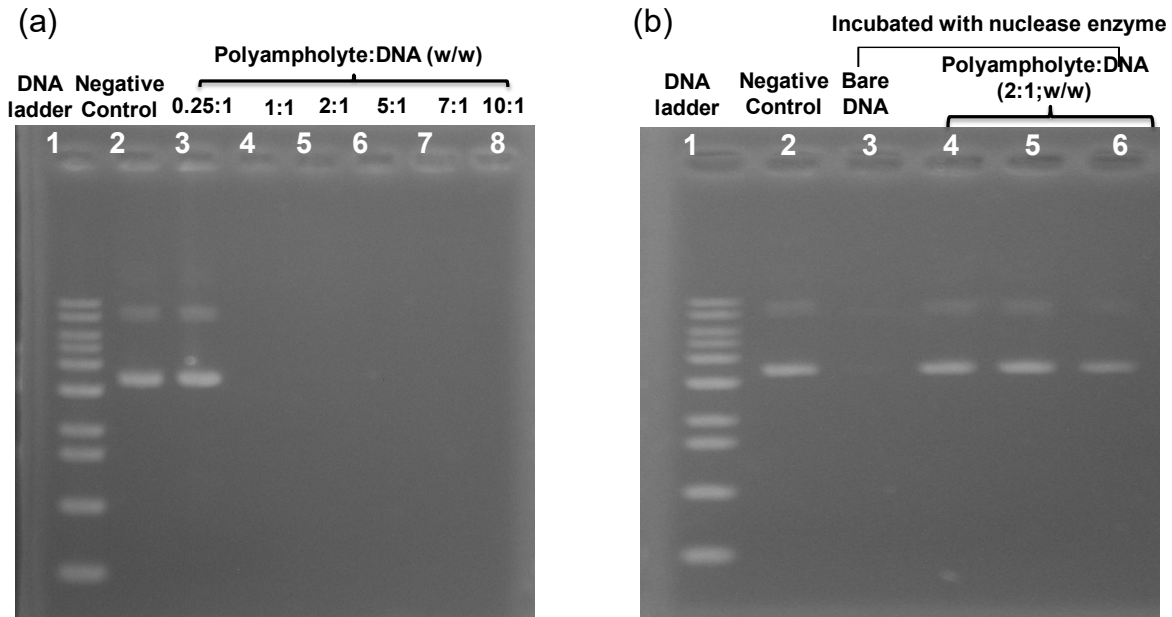


Figure 3. Agarose gel electrophoresis studies. (a) Complex formation between polyampholyte and pDNA. The amount of plasmid DNA was fixed at 1 μg , and the complexes were prepared using different amount of PEI-BSA in PBS (-). Lane-1; 1 kb DNA ladder, Lane 2; pDNA as a negative control, Lanes 3- 8; PEI-BSA/pDNA complexes at different mass ratios 0.25:1, 1:1; 2:1, 5:1,7:1 and 10:1 (b) Protection of pDNA within the PEI-BSA/pDNA complex against nuclease activity. Lane 1; 1 kb DNA ladder, Lane 2;pDNA as a negative control, Lane 3;pDNA alone incubated with DNase I at 0.1 U/ μg DNA for 30 min; Lanes 4-6;PEI-BSA:pDNA (2:1 w/w) was incubated with different amounts of DNase I at 0.1, 0.2, or 0.4 U/ μg DNA for 30 min. After treatment with DNase I the enzyme was deactivated by adding EDTA and subsequently heparin was added to each sample before agarose gel electrophoresis.

3.3.4.2 Stability against nucleases

It is important for carriers to protect pDNA from enzymatic degradation in order to be able to efficiently release the DNA for gene expression, both *in vitro* as well as *in vivo*. To investigate the stability of DNA loaded PEI-BSA against enzymatic degradation, we examined the ability of PEI-BSA to protect pDNA from DNase I-induced digestion at 37°C. Following incubation with DNase I, we used heparin to disrupt the PEI-BSA-pDNA complex to release pDNA. In this case, heparin serves to competitively displace polycations (such as amine groups in PEI-BSA) from the pDNA. As shown in Figure 3b, incubation of uncomplexed pDNA with DNase I at 0.1 U/μg for 30 min resulted in complete digestion of the pDNA. In contrast, following incubation of the PEI-BSA-pDNA complex (2:1 w/w ratio) with increasing concentrations of DNase I (0.1, 0.2, or 0.4 U/μg) pDNA could still be readily released from the PEI-BSA-pDNA complex demonstrating that PEI-BSA protects the pDNA cargo from enzymatic degradation.

3.4 Cytotoxicity assay

The *in vitro* toxicities of different polymers were measured as a function of polymer concentration using the LDH cytotoxicity assay kit. The lactate dehydrogenase (LDH) assay measure the release of the LDH enzyme from cells. The principle is that lactate dehydrogenase is normally localized in the cytoplasm and is released into the culture medium when cells are irreversibly damaged; the release therefore acts as an indicator of cell death. LDH activity is measured by an increase in colorimetric signal. Figure 4 demonstrates the cell viability of different polymer samples at different concentrations after 24 h treatment. Branched PEI (25 kDa) had the highest toxicity whereas PEI-SA and PEI-BSA were less toxic. The cell viabilities in cells treated with PEI-SA and PEI-BSA were greater than 70% at a concentration of 10 μg/mL, while the cell viability in cells treated with PEI was just 55%. Branched PEI (25 kDa) has been previously reported to have high cell toxicity³⁹. PEI toxicity appears to be mainly associated with the high net

positive charge on the polymer due to the numerous amino groups present in the polymeric backbone (Figure 4). The reduced toxicity of PEI-SA or PEI-BSA compared to PEI likely arises as a result of the modifications that reduce the number of amine groups in the polymer backbone. These data align with previous reports where modification of branched PEI has been shown to decrease polymer toxicity²⁹⁻³². In addition, these data further support the use of PEI-BSA as a low-toxicity gene delivery vehicle.

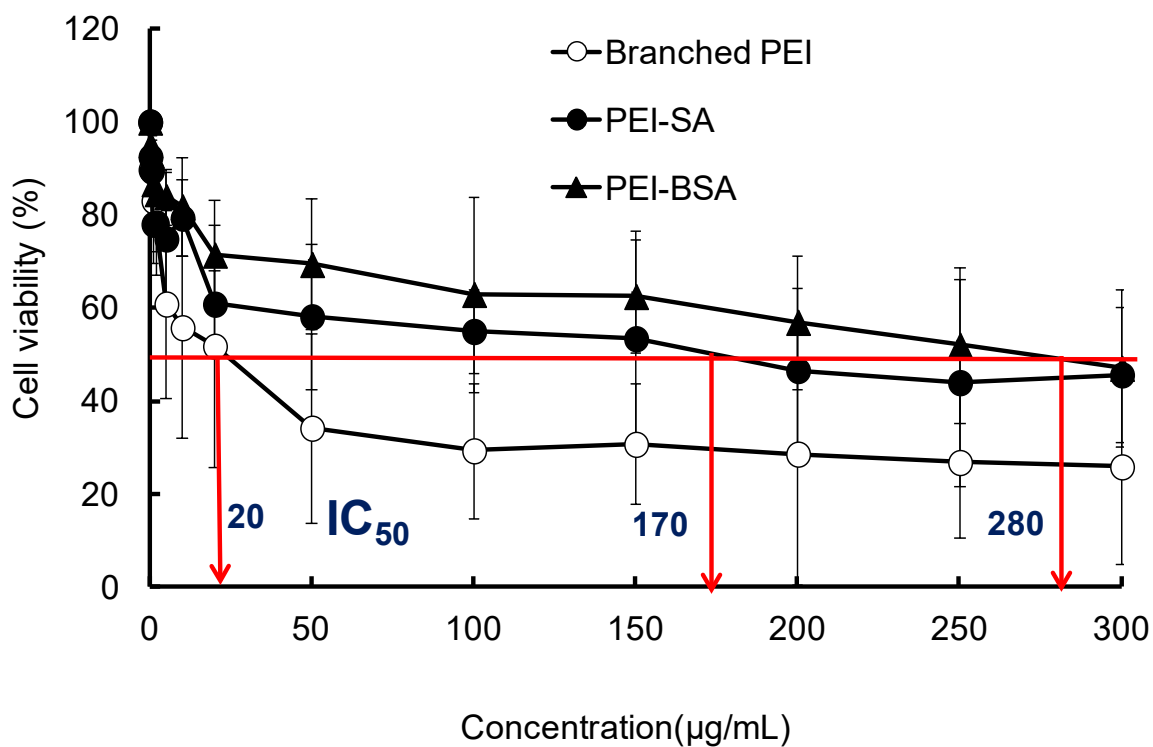


Figure 4. HEK-293T cells were incubated with different concentrations of branched PEI, PEI-SA, or PEI-BSA for 24 h, followed by LDH cytotoxicity assay analysis. The IC₅₀ represents the concentration of polyampholyte that caused a 50% reduction in cell viability of a treated cell culture compared to an untreated control culture; data are expressed as the mean ± standard deviation (SD)

3.5 Enhancement of gene delivery using freeze concentration

3.5.1 Cell freezing with polyampholyte-DNA complexes

In this study, we elected to use HEK-293T cells for transfection studies because they contain the SV40 large T antigen, which allows for substantial replication of transfected plasmids⁴⁰. To demonstrate the effect of freezing on transfection, HEK-293T cells were frozen in the presence of increasing amounts of PEI-BSA along with a fixed quantity of pDNA (1 μ g) to give PEI-BSA:pDNA (w/w) ratios of 2:1, 5:1, 7:1, and 10:1 in the presence of 10% PLL-SA as a cryoprotectant. The final freezing volume was 50 μ L in PBS(-). The commercially available transfection reagents jetPEI[®] and Lipofectamine 3000 were also used as a comparison. As illustrated in Figure S5, cell survival was greater than 90% in the presence of the polymeric cryoprotectant 10% PLL-SA. Next, we investigated the adsorption of cyanine-3 (Cy-3)-labeled pDNA(1 μ g) complexes to the cell membrane to compare the freeze concentration method versus the non-freezing method, along with a comparison between the commercially available transfection reagent jetPEI[®](2 μ g)and PEI-BSA(2 μ g). As shown in Figure S6a, enhanced adsorption of Cy-3 labeled-pDNA was found when the freeze concentration approach was used for jetPEI[®] compared to the non-frozen method. Similarly, enhanced adsorption of Cy-3-labeled pDNA was evident when the freeze concentration approach was used for PEI-BSA (Figure S6b) compared to the non-frozen method. The Cy-3 fluorescence intensity was quantitated using confocal microscopy. In addition to confirming that the freeze concentration method increases Cy-3 pDNA adsorption to HEK-293T cells compared to the non-frozen method, we also showed that PEI-BSA allowed for better Cy3 pDNA adsorption to cells than jetPEI[®] (Figure S6c). Taken together, these data indicate that freezing enhances the level of polymer:pDNA complexes around

the cell membrane and that PEI-BSA was more effective as a carrier than jetPEI[®]. One possible explanation for this difference is the fact that PEI-BSA, which contains a hydrophobic alkyl group, could more effectively interact with the cell membrane via hydrophobic interactions. These data are consistent with prior studies that demonstrated effective adsorption of materials using this freeze concentration approach^{10, 11}.

3.5.2 Transfection studies using confocal microscopy

An *in vitro* transfection process was then evaluated using pDNA encoding GFP as a reporter gene. To perform this, we cryopreserved HEK-293T cells with nanocarrier-pDNA complexes in the presence of the polymeric cryoprotectant 10% PLL-SA for 24 h. After thawing, the cell suspension was seeded onto the bottom of a glass dish and then incubated for a further 10 h. In order to compare with the non-frozen method, nanocarrier-pDNA complexes were gently added directly to HEK-293T cells seeded on the bottom of a glass dish and these were also incubated for a further 10 h. GFP expression was examined using CLSM. Transfection studies were first performed using the commercially available cationic carriers jetPEI[®] and Lipofectamine 3000. JetPEI[®] is a linear PEI derivative that is well suited for plasmid DNA delivery, whereas Lipofectamine 3000 is a lipid-based transfection agent generally regarded as a highly efficient gene transfection reagent. As shown in Figure 5 a, bHEK-293T cells transfected with GFP using the freeze concentration method had significantly better GFP expression than cells transfected using the non-frozen method, which showed barely any GFP expression, regardless of which of the commercial carriers was used. One possible explanation for this is that the freezing process likely increases the concentration of carrier-pDNA system in the environment around the cell membrane, after which the carrier-pDNA can enter the cell rather than diffusing away from the cells. Previous work from our group also indicates that freeze concentration may have a beneficial

effect on protein internalization^{10,11}. We also used the same experimental approach to examine the effect of both branched PEI and PEI-BSA as carriers during transfection of HEK-293T cells with a pDNA encoding GFP to allow a comparison with the commercially available carriers. A branched PEI:pDNA complex (5:1 w/w ratio) and several different PEI-BSA:pDNA complexes (2:1, 5:1, 7:1, and 10:1 w/w ratios) were used under freeze concentration and non-frozen conditions. Figure 5c-g shows the confocal images for GFP expression. The use of branched PEI as a carrier resulted in a low level of GFP expression regardless of whether freezing was used (Figure 5c). In contrast, the transfection efficiency was significantly higher when PEI-BSA was used as carrier, and was even more pronounced under freeze concentration conditions (Figure 5d). Interestingly, as the ratio of PEI-BSA:pDNA increased from 2:1 to 5:1, the gene transfection efficiency increased but further increases in the PEI-BSA:pDNA ratio (7:1 to 10:1) appeared to cause a decrease in expression (Figure 5f,g). The reason for this is not known. It has been known from the literature that branched PEI is considered to be a good transfection carrier⁴¹. Because of positive charge, PEI increases endocytosis due to an electrostatic interaction with the cell membrane. However, there are also reports that suggest that less positively charged²⁹ even or negatively charged polymer-DNA complexes undergo efficient transfection⁴². Moreover, we also evaluated the effect of 10% PLL-SA cryoprotectant alone in the non-frozen condition to evaluate the effect on transfection. Figure S7 (a-g) shows confocal images following transfections in the presence of cryoprotectant under non-frozen conditions, compared with the frozen conditions, using all commercial available transfection carriers and PEI-BSA. These results show that uniformly there was almost no fluorescence observed in cells in the unfrozen conditions compared with the frozen condition. The efficiency of transfection in the non-frozen system in the presence of cryoprotectant was almost identical to that seen in the absence of cryoprotectant. These results suggest that the

polyampholyte cryoprotectant alone does not affect transfection under normal conditions. However under frozen conditions, the polyampholyte cryoprotectant has a unique property of increasing the concentration of solutes, as we have previously reported.^{10, 34}

Regardless, in our study, modified PEI was found to be a better transfection carrier than branched PEI in our frozen system. As these data were largely qualitative, we next sought to quantify the gene transfection efficiency in our system more precisely using luciferase as a reporter rather than GFP.

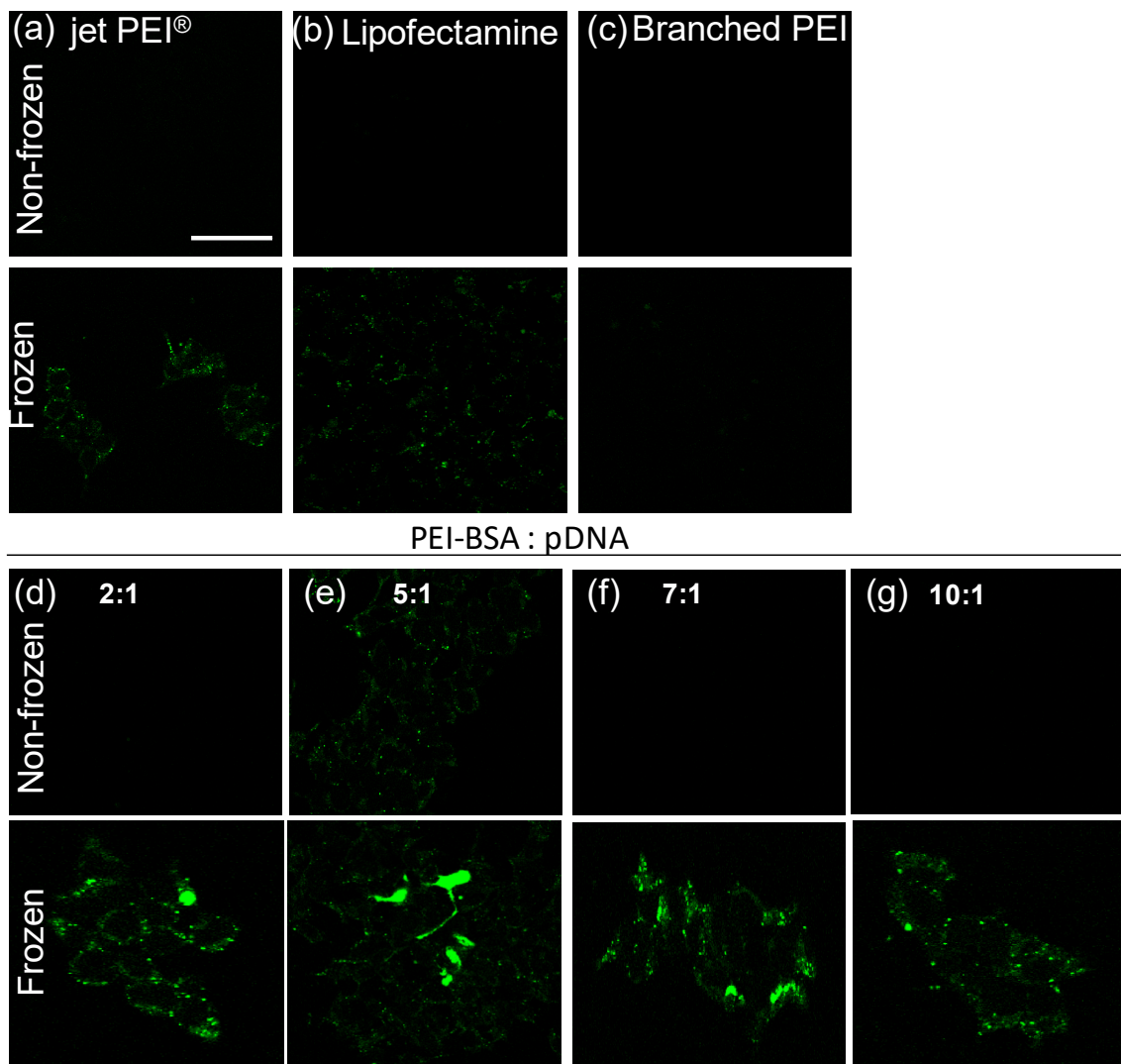


Figure 5. Comparison of the *in vitro* transfection efficiency of different pDNA complexes in HEK-293T cells using a pDNA encoding GFP. HEK-293T cells were either frozen in the presence of the different pDNA complexes along with 10% PLL-SA as a cryoprotectant (Frozen) or the pDNA complexes were added directly to the cells without freezing (Non-frozen) and were incubated for 10 h. Each commercially available transfection reagent was incubated with plasmid DNA (1 µg) (a) jetPEI[®] (b) Lipofectamine 3000 (c) Branched PEI, and PEI-BSA:pDNA ((d) 2:1, (e) 5:1, (f) 7:1, (g) 10:1, w/w). Confocal microscopy images showing GFP expression are shown. Scale bars: 50 µm.

3.5.3 Luciferase expression of unfrozen and frozen system

The experimental conditions used to analyze gene transfection efficiency using luciferase were modified slightly compared to the GFP study. For GFP expression, cells were cultured for 10 h post-plating (and post-transfection) to allow for expression of GFP to evaluate transfection efficiency. However, for luciferase expression, cells were transfected with the pGL4.51 plasmid (which contains the luciferase gene) and were cultured for at least 48 h to allow for sufficient enzyme expression to occur. As for the GFP experiment, complexes of jetPEI[®] and Lipofectamine 3000, a complex of branched PEI (5:1 ratio w/w), and several different PEI-BSA complexes (2:1, 5:1, 7:1, and 10:1 w/w ratios) were evaluated under freeze concentration and non-frozen conditions. As shown in Figure 6, luciferase reporter gene expression was significantly higher using the freeze concentration method, compared to the non-frozen method for all transfection carriers. Freeze concentration resulted in an almost 10-fold enhancement in luciferase expression for both jetPEI[®] and Lipofectamine 3000. This result confirmed our previous finding for GFP, namely that freeze concentration increased the transfection efficiency of both carriers. Surprisingly, jetPEI[®] luciferase expression was found to be higher than Lipofectamine 3000 in both the non-frozen and freeze

concentration conditions. Other studies have reported that jetPEI[®] can provide a higher transfection efficiency compared to Lipofectamine^{43,44}. One possible reason for the reduced transfection efficiency of Lipofectamine 3000 compared to jetPEI[®] is that it can adsorb onto large anionic serum protein aggregates. These large aggregates most likely will not be able to cross the cell membrane and deliver pDNA to the cells⁴⁵; it is possible that pDNA-jetPEI[®] could prevent this aggregation. Another possible reason for this difference is that, depending on the carrier, there might be differences in how efficiently different intracellular processes such as nuclear translocation or integration of a vector into chromosomal DNA occur. In this study, we did not examine these factors but our future studies will focus on understanding these different transfection efficiencies.

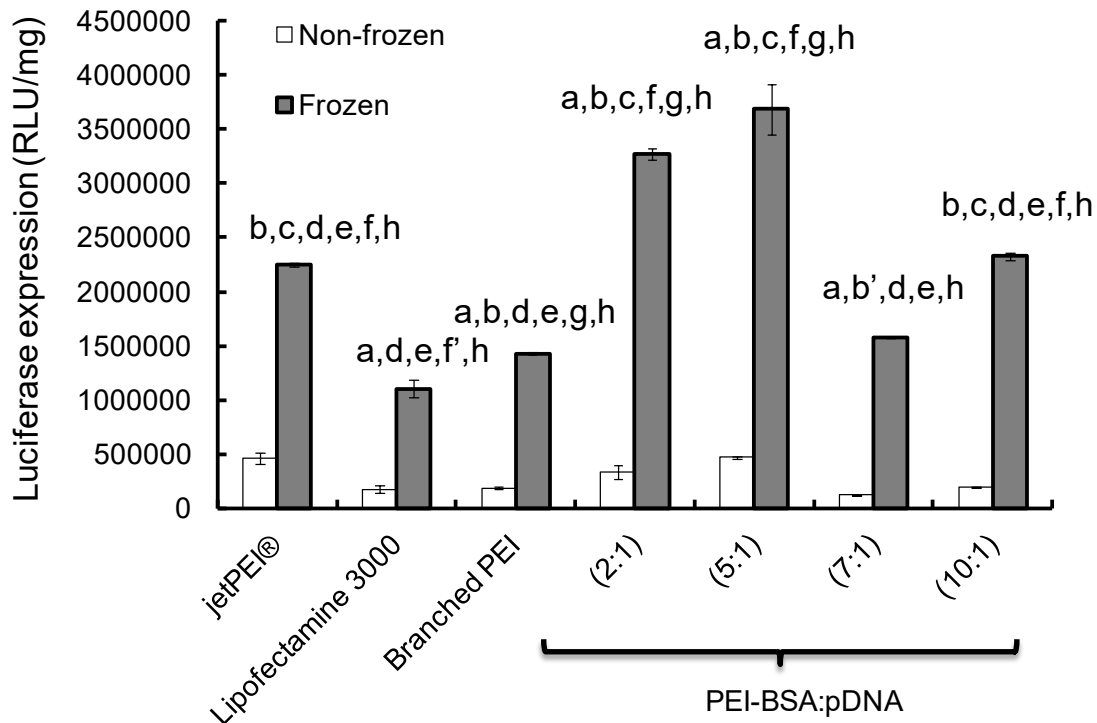


Figure 6. Comparison of the *in vitro* transfection efficiency of different pDNA complexes in HEK-293T cells using a pDNA encoding luciferase. HEK-293T cells were either frozen in the presence

of the different pDNA complexes along with 10% PLL-SA as a cryoprotectant (Frozen) or the pDNA complexes were added directly to the cells without freezing (Non-frozen). Luciferase expression was measured using a luminometer 48 hours later. The pDNA(1 μ g) was complexed with either jetPEI[®], Lipofectamine 3000, Branched PEI, or PEI-BSA:pDNA (at various ratios of 2:1, 5:1, 7:1, or 10:1, w/w). White bar: Non-frozen; grey bar: Frozen. Data are expressed as the mean \pm standard deviation (SD). a: $p < 0.01$ vs. Jet PEI[®], b: $p < 0.01$ vs. Lipofectamine 3000, b': $p < 0.05$ vs. Lipofectamine 3000, c: $p < 0.01$ vs. branched PEI, d: $p < 0.01$ vs. PEI-BSA:DNA (2:1), e: $p < 0.01$ vs. (5:1), f: $p < 0.01$ vs. (7:1), f': $p < 0.05$ vs. (7:1), g: $p < 0.01$ vs. (10:1), and h: $p < 0.01$ vs. corresponding non-frozen condition.

Figure 6 also shows that HEK-293T cells treated with PEI-BSA had significantly enhanced luciferase expression (approximately 10-fold) using the freeze concentration method compared to cells treated using the non-frozen method. In particular, the transfection efficiencies of PEI-BSA:pDNA at ratios of 2:1 and 5:1 (w/w) were significantly higher than at ratios of 7:1 and 10:1, consistent with the GFP experiment (compare Figure 6 with Figure 5d-g). This difference in transfection efficiency might arise as a result of less binding of PEI-BSA to pDNA. When the PEI-BSA:pDNA (w/w) ratio was greater than 5:1, the increased positive charge on the polymer will likely result in a stable complex with the pDNA, making it more difficult to dissociate the PEI-BSA-pDNA complex. As a result, this may cause a reduction in transfection efficiency. These results, therefore, demonstrate that effective gene delivery is dependent on the ratio of PEI-BSA to pDNA using both the frozen and non-frozen methods. Another point of interest is that at 10:1 (PEI-BSA:pDNA, w/w), luciferase expression increased compared with that at 7:1 (PEI-BSA:pDNA, w/w) (Figure 6). In addition, as was seen in the GFP experiment, the efficiencies of

the luciferase transfections using branched PEI were lower than for PEI-BSA using both the non-frozen and the frozen methods (Figure 6). Overall, as expected, freeze concentration increased luciferase expression in a similar manner to that which was observed in the GFP transfection studies (Figure 5a-g).

Gabrielson and co-workers demonstrated enhanced transfection efficiency after using of acetylated PEI, which they attributed to weak binding between the acetylated PEI and pDNA. They also demonstrated that acetylated PEI releases more pDNA than branched PEI using a heparin displacement assay⁴⁶. Zintchenko et al. have also shown that modification of branched PEI with succinic anhydride displayed a high efficiency in siRNA-mediated knockdown of a target gene compared with branched PEI 25kDa²⁹.

Forrest et al. have also shown that partial acetylation of PEI also enhances gene transfection efficiency⁴⁷. These reports are complementary to our data. Nevertheless, in our present study, PEI-BSA produced significantly much better transfection efficiency than the commercially available carriers jetPEI[®] and Lipofectamine 3000. Our data also suggest that there is an optimal ratio of PEI-BSA to DNA that should be determined in order to enhance transfection efficiency. Finally, our results also demonstrated the considerable enhancement in transfection efficiency is obtained when the freeze concentration method is combined with PEI-BSA and suggests that this approach has the potential to be used as an efficient gene delivery system *in vitro*.

3.5.4 Intracellular distribution of polyampholytes-pDNA complex

For an effective transfection method to be useful in therapeutic applications, it is important that the transfection system facilitates the escape of pDNA from the endosome and allow for its efficient transfer to the nucleus. Therefore, we next sought to understand the endosomal escape

capability of our transfection system. To study this, we used confocal microscopy to observe the intracellular localization of the polyampholytes. To achieve this, plasmid pAcGFP1-N2 was labeled with Cy3 dye and the endosomes were stained with LysoTracker Green while cell nuclei were stained with Hoechst 33342. In order to observe the intracellular distribution of pDNA after freeze concentration, the thawed HEK-293T cell suspensions were seeded into plates and cultured for 24 h. As shown in Figure 7a, Cy3-pDNA was still present in endosomes in the case of the branched PEI-DNA (2:1, w/w) complex as evidenced by the yellow color. In fact, the majority of Cy-3-pDNA was present in endosomes and only a very small amount of pDNA was released. In contrast, in the case of PEI-BSA-pDNA complexes (2:1, w/w), more pDNA was clearly visible in the cytoplasm, with much lower levels being evident in the endosome (Figure 7b). This data indicated that pDNA was efficiently released from endosomes when PEI-BSA was used. The most probable reason for this enhanced release of pDNA from polyampholytes is due to weaker binding between pDNA and the polyampholyte resulting in more efficient release of pDNA. Therefore, one of the other reasons for there being enhanced transfection efficiency with PEI-BSA might be because of this reduced binding between the polyampholyte and pDNA leading to facile unpackaging of the pDNA. In contrast, branched PEI might be expected to exhibit a strong interaction with pDNA and this will tend to reduce the transfection efficiency.

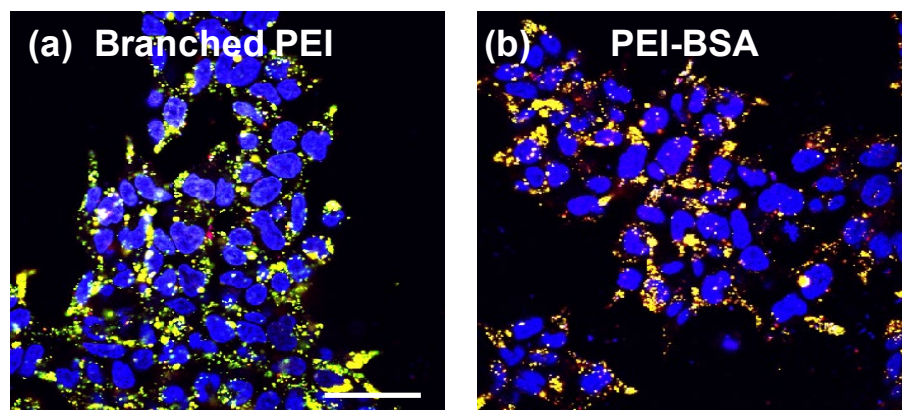


Figure 7. Intracellular localization of Cy-3 labeled pDNA in HEK293T cells. HEK293T cells (1×10^6 cells) were cryopreserved in the presence of polymeric cryoprotectant (10% PLL-SA) and Cy-3-labeled pDNA (1 μ g). The cells were thawed and seeded for 24 h at 37°C. Following this, the endosomes/lysosomes and nuclei were stained using LysoTracker Green and Hoechst blue 33342, respectively. (a) Branched PEI: DNA (2:1, w/w) (b) PEI-BSA (2:1,w/w). Scale bar: 50 μ m.

Various hypotheses explaining endosomal escape has been proposed over the past few years. Branched PEI 25kDais thought to be an effective transfection agent due to the ‘proton sponge’ hypothesis, which is thought to facilitate the escape of complexes from endosomes. According to this hypothesis, polymers with pKa values between neutral and endosomal pH, such as PEI, have the ability to buffer the ATPase-mediated acidification of endocytic vesicles. In PEI, every third atom of PEI is a nitrogen that could be potentially protonated, thereby providing a strong buffering capacity. A relatively large number of protons may therefore accumulate in the endocytic vesicles. The influx of positive charge (hydrogen ions) would have to be balanced by an influx of counterions (primarily chloride) leading to endosome swelling, rupture of the endosome membrane, and eventual release of the DNA into the cytosol. However, this proposed mechanism is controversial, since a recent study did not observe any change in endosomal pH after exposure to PEI over a 24 h period⁴⁸.

Recently, numerous studies have shown that efficient transfer of DNA inside the cell might arise as a result of a weak interaction between the carrier and DNA in the endosome allowing for the subsequent release of DNA into the cytoplasm and a resultant increase in transfection efficiency^{46,47,49}. Similar work to ours has been performed by Uludag et al., in which they showed

that branched PEI modified by either oleic acid or stearic acid gave enhanced transfection efficiency compared with commercially available transfection reagents⁴⁹. Other reports, also similar to ours, have shown that the presence of long alkyl chains in the carrier would be expected to strengthen the interaction with the cell membrane, increasing endocytosis and thereby also enhancing the transfection efficiency⁵⁰⁻⁵³. With regard to endosome escape, we have shown that PEI-BSA:pDNA complex could efficiently escape from endosomes also resulting in increased transfection efficiency with low toxicity. However, the mechanism for efficient endosome escape to the cytoplasm is not yet fully understood, but we believe that it is due to weak binding between the polymer carrier and pDNA. In addition, the use of freeze concentration to further enhance transfection efficiency may prove to be extremely useful for gene delivery *in vitro*. Our data clearly indicate that, after freeze concentration, polyampholytes were capable of enhancing DNA escape from endosomes, which will also enhance transfection efficiency. We think it will be extremely important to elucidate the exact mechanism of endosomal escape that occurs after using the freeze concentration method and we plan to investigate this in the near future.

4. CONCLUSIONS

In this study, we demonstrated the effective use of a freeze concentration method as part of a cell transfection system. We found that freeze concentration accelerates and enhances gene expression and is an additional facile procedure even when used with currently available transfection reagents, such as jetPEI[®] or Lipofectamine 3000. Furthermore, we also developed new self-assembling polyampholytes as non-viral carriers. These polyampholytes were extremely small in size, were able to condense DNA efficiently, and were found to be much less toxic compared to branched PEI. In HEK-293T cells, confocal microscopy analysis of transfected GFP expression and direct luciferase activity measurements revealed that maximum transfection

efficiency depends on the appropriate polyampholyte:DNA ratio and is enhanced using the freeze concentration method. These findings provide an effective, simple, and non-toxic approach for enhancing gene delivery. The present studies suggest that the unique combination of a polyampholyte non-viral carrier and a physical method such as freeze concentration might be a safe and efficient system for *in vitro* gene delivery. Further work should focus on evaluating the use of this system in clinically relevant studies to assess its potential as a system for the treatment of genetic diseases.

ASSOCIATED CONTENT

Supporting Information

Synthesis of polyampholyte cryoprotectant, ^1H NMR of cryoprotective polyampholytes, ^1H NMR of modified branched PEI, detailed analysis by XPS, CAC of branched PEI, adsorption of Cy-3 labeled DNA to cells to compare non-frozen and frozen systems and quantification through measurement of fluorescent intensity. Supplementary data related to this article can be found at <http://pubs.acs.org>.

AUTHOR INFORMATION

Corresponding Author

*E-mail: mkazuaki@jaist.ac.jp

Notes: The authors declare no competing financial interest.

Author Contributions

The manuscript was written through contributions of all authors. All authors have given approval to the final version of the manuscript.

Funding Sources

This study was supported in part by a Grant-in-Aid, KAKENHI (16K12895), for scientific research from Japan Society for the Promotion of Science, and in part by a Grant-in-Aid for Scientific Research on Innovative Areas (JP25102006) from the Ministry of Education, Culture, Sports, Science, and Technology, Japan.

Notes

The authors have no conflicts of interest to declare.

REFERENCES

1. Chen, J.; Guo, Z.; Tian, H.; Chen, X. Production and Clinical Development of Nanoparticles for Gene Delivery. *Mol. Ther. Methods Clin. Dev.* **2016**, *3*, 1–8.
2. Manjila, S. B.; Baby, J. N.; Bijin, E. N.; Constantine, I.; Pramod, K.; Valsalakumari, J. Novel Gene Delivery Systems. *Int. J. Pharm. Investig.* **2013**, *3*, 1–7.
3. Dizaj, S. M.; Jafari, S.; Khosroushahi, A. Y. A Sight on the Current Nanoparticle-based Gene Delivery Vectors. *Nanoscale Res. Lett.* **2014**, *9*, 252–260.
4. Nayerossadat, N.; Maedeh, T.; Ali, P. A. Viral and Nonviral Delivery Systems for Gene Delivery. *Adv. Biomed. Res.* **2012**, *1*, 1-30.

5. Thomas, C. E.; Ehrhardt, A.; Kay, M. A. Progress and Problems with the Use of Viral Vectors for Gene Therapy. *Nat. Rev. Genet.***2003**, *4*, 346–358.
6. Zhou, R.; Norton, J. E.; Dean, D. A. Electroporation-mediated Gene Delivery to the Lungs. *Methods Mol. Biol.***2008**, *423*, 233–247.
7. Zhang, Y.; Tachibana, R.; Okamoto, A.; Azuma, T.; Sasaki, A.; Yoshinaka, K.; Tei, Y.; Takagi, S.; Matsumoto, Y. Ultrasound-mediated Gene Transfection *in vitro*: Effect of Ultrasonic Parameters on Efficiency and Cell Viability. *Int. J. Hyperthermia***2012**, *28*, 290–299.
8. Aravindaram, K.; Yang, N. S. Gene Gun Delivery Systems for Cancer Vaccine Approaches. *Methods Mol. Biol.***2009**, *542*, 167–178.
9. Beebe, S. J.; Sain, N. M.; Ren, W. Induction of Cell Death Mechanisms and Apoptosis by Nanosecond Pulsed Electric Fields (nsPEFs). *Cells***2013**, *2*, 136–162.
10. Ahmed, S.; Hayashi, F.; Nagashima, T.; Matsumura, K. Protein Cytoplasmic Delivery Using Polyampholyte Nanoparticles and Freeze Concentration. *Biomaterials***2014**, *35*, 6508–18.
11. Ahmed, S.; Fujita, S.; Matsumura, K. Enhanced Protein Internalization and Efficient Endosomal Escape using Polyampholyte-modified Liposomes and Freeze Concentration. *Nanoscale***2016**, *8*, 15888–15901.
12. Bhatnagar, B. S.; Pikal, M. J.; Bogner, R. H. Study of the Individual Contribution of Ice Formation and Freeze-concentration on Isothermal Stability of Lactate Dehydrogenase During Freezing. *J. Pharm. Sci.***2008**, *97*, 798–814.
13. Pham, Q.T. Advances in food freezing/thawing/freeze concentration modelling and techniques. *Jpn. J. Food Eng.* **2008**, *9*, 21–32.

14. Sanchez, J.; Ruiz, Y.; Auleda, J. M.; Hernandez, E.; Reventos, M. Freeze Concentration in the Fruit Juices Industry. *Food Sci. Technol. Int.* **2009**, *15*, 303–315.
15. Kiani, H.; Sun, D. W. Water crystallization and its importance to freezing of foods. *Trends Food Sci. Technol.* **2011**, *22*, 407–426.
16. Kawakami, S.; Higuchi, Y.; Hashida, M. Nonviral approaches for targeted delivery of plasmid DNA and oligonucleotides. *J. Pharm. Sci.* **2008**, *97*, 726-745.
17. Rush, A.M.; Thompson, M.P.; Tatso, E.T.; Gianneschi, N.C. Nuclease-resistant DNA via high density packing in polymeric micellar nanoparticles coronas. *ACS Nano*, **2013**, *7*(2), 1379-1387.
18. Luo, D.; Saltzman, W. M. Synthetic DNA Delivery Systems. *Nature Biotechnol.* **2000**, *18*, 33–37.
19. Pezzoli, D.; Kajaste-Rudnitski, A.; Chiesa, R.; Candiani, G. Lipid-based Nanoparticles as Nonviral Gene Delivery Vectors. *Methods Mol. Biol.* **2013**, *1025*, 269–279.
20. Chen, J.; Guo, Z.; Tian, H.; Chen, X. Production and clinical development of nanoparticles for gene delivery. *Mol Ther Methods Clin Dev.* **2016**, *3*, 1-8.
21. Liu, G.; Swierczewskaa, M.; Lee, S.; Chen, X. Functional Nanoparticles for Molecular Imaging Guided Gene Delivery. *Nano Today* **2010**, *5*, 524–539.
22. Lungwitz, U.; Breunig, M.; Blunk, T.; Gopferich, A. Polyethyleneimine-based Non-viral Gene Delivery Systems. *Eur. J. Pharm. Biopharm.* **2005**, *60*, 247–266.

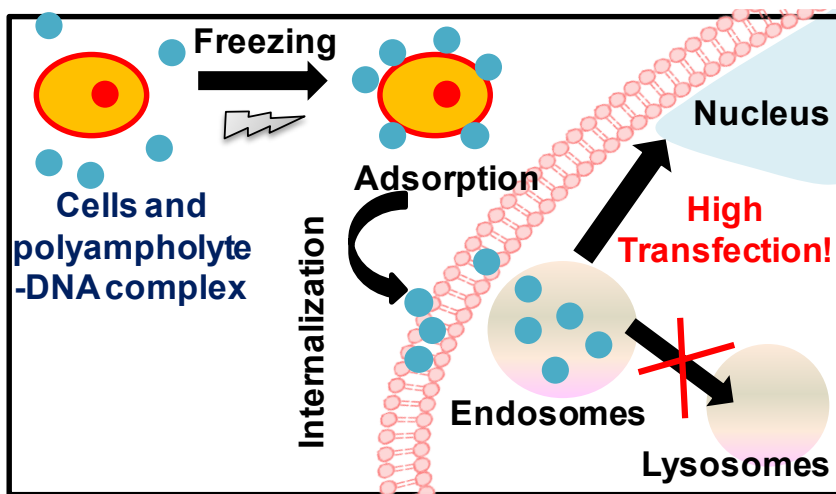
23. Zhou, D.; Li, C.; Hu, Y.; Zhou, H.; Chen, J.; Zhang, Z.; Guo, T. PLL/pDNA/P(His-co-DMAEL) Ternary Complexes: Assembly, Stability and Gene Delivery. *J. Mater. Chem.* **2012**, *22*, 10743–10775.
24. Oliveira, H.; Pires, L. R.; Fernandez, R.; Martins, M. C.; Simoes, S.; Pego, A. P. Chitosan-based Gene Delivery Vectors Targeted to the Peripheral Nervous System. *J. Biomed. Mater. Res. A.* **2010**, *95*, 801–810.
25. Huang, R.; Ke, W.; Liu, Y.; Jiang, C.; Pie, Y. The Use of Lactoferrin as a Ligand for Targeting the Polyamidoamine-based Gene Delivery System to the Brain. *Biomaterials* **2008**, *29*, 238–246.
26. Tamboli, V.; Mishra, G. P.; Mitra, A. K. Polymeric Vectors for Ocular Gene Delivery. *Ther. Deliv.* **2011**, *2*, 523–536.
27. Varkouhi, A. K.; Scholte, M.; Storm, G.; Haisma, H. J. Endosomal escape pathways for delivery of biologicals. *J. Control. Release* **2010**, *151*, 220–228.
28. Moghimi, S. M.; Symonds, P.; Murray, J. C.; Hunter, A. C.; Debska, G.; Szewczyk, A. A Two-stage Poly (ethylenimine)-mediated Cytotoxicity: Implication for Gene Transfer/Therapy. *Mol. Ther.* **2005**, *11*, 990–995.
29. Zintchenko, A.; Philipp, A.; Dehshahri, A.; Wagner, E. Simple modification of branched PEI Lead to Highly Efficient siRNA Carriers with Low Toxicity, *Bioconjugate Chem.* **2008**, *19*, 1448–1455.
30. Zhang, Q. F.; Lua, C. R.; Yin, D. X.; Zhang, J.; Liu, Y. H.; Peng, Q.; Xu, Y.; Yu, X. Q. Amino Acid-modified Gene Delivery Efficiency and Biocompatibility. *Polymers* **2015**, *7*, 2316–2331.

31. Hu, Y. L.; Zhou, D. Z.; Li, C. X.; Zhou, H.; Chen, J. T.; Zhang, Z. P.; Guo, T. Y. Gene Delivery of PEI Incorporating with Functional Block Copolymer Via Non-covalent Assembly Strategy. *Acta Biomater.* **2013**, *9*, 5003–5012.
32. Englert, C.; Fevre, M.; Wojtecki, R.J.; Cheng, W.; Xu, Q.; Yang, C.; Ke, X.; Hartlieb, M.; Kempe, K.; Garcia, J. M.; Ono, R. J.; Schubert, U. S.; Yang, Y. Y.; Hedrick, J. L. Facile Carbohydrate-mimetic Modifications of Poly(ethyleneimine) Carriers for Gene Delivery Applications. *Polym. Chem.* **2016**, *7*, 5862–5872.
33. De Jong, W. H.; Borm, P. J. Drug Delivery and Nanoparticles: Applications and Hazards. *Int. J. Nanomedicine* **2008**, *3*, 133–149.
34. Matsumura, K.; Hyon, S. H. Polyampholytes as Low Toxic Efficient Cryoprotective Agents with Antifreeze Protein Properties. *Biomaterials* **2009**, *30*, 4842–4849.
35. Matsumura, K.; Kawamoto, K.; Takeuchi, M.; Yoshimura, S.; Tanaka, D.; Hyon, S. H. Cryopreservation of a Two Dimensional Monolayer Using a Slow Vitrification Method with Polyampholyte to Inhibit Ice Crystal Formation. *ACS Biomater. Sci. Eng.* **2016**, *2*, 1023–1029.
36. Matsumura, K.; Hayashi, F.; Nagashima, T.; Hyon, S. H. Long-term Cryopreservation of Human Mesenchymal Stem Cells using Carboxylated Poly-L-lysine Without the Addition of Proteins or Dimethyl Sulfoxide. *J. Biomater. Sci. Polym. Ed.* **2013**, *24*, 1484–1497.
37. Read, M.L.; Singh, S.; Ahmed, Z.; Stevenson, M.; Briggs, S. S.; Oupicky, D.; Barrett, L. B.; Spice, R.; Kendall, M.; Berry, M.; Preece, J. A.; Logan, A.; Seymour, L. W. A Versatile Reducible Polycation-based System for Efficient Delivery of a Broad Range of Nucleic Acids. *Nucleic Acids Res.* **2005**, *33*, e86.

38. Shang, L.; Nienhaus, K.; Nienhaus, G. U. Engineered Nanoparticles Interacting with Cells: Size Matters. *J Nanobiotechnology***2014**, *12*, 1–11.
39. Kafil, V.; Omid, Y. Cytotoxic Impacts of Linear and Branched Polyethyleneimine Nanostructures in A431 cells. *Bioimpacts***2011**, *1*, 23–30.
40. Mahon, M.J. Vectors Bicistronically Linking a Gene of Interest to the SV40 Large T Antigen in Combination with the SV40 Origin of Replication Enhance Transient Protein Expression and Luciferase Reporter Activity. *BioTechniques***2011**, *51*, 119–128.
41. Dong, W.; Li, S.; Jin, G.; Sun, Q.; Ma, D.; Hua, Z. Efficient Gene Transfection into Mammalian Cells Mediated by Cross-linked Polyethyleneimine. *Int. J. Mol. Sci.***2007**, *8*, 81-102.
42. Wyrwal, M.; Leduc, C.; Sarna, M.; Goncalves, C.; Kepczynski, M.; Midoux, P.; Nowakowska, M.; Pichon, C. Gene delivery efficiency and intracellular trafficking of novel poly(allylamine) derivatives. *Int. J. Pharm.***2015**, *478*, 372-382.
43. Yamano, S.; Dai, J.; Moursi, A. M. Comparison of Transfection Efficiency of Nonviral Gene Transfer Reagents. *Mol. Biotechnol.***2010**, *46*, 287–300.
44. Lehner, R.; Wang, X.; Hunziker, P. Plasmid Linearization Changes Shape and Efficiency of Transfection Complexes. *Eur. J. Nanomed.* **2013**, *5*, 205–212.
45. Zou, W.; Liu, C.; Chen, Z.; Zhang, N. Preparation and Characterization of Cationic PLA-PEG Nanoparticles for Delivery of Plasmid DNA. *Nanoscale Res. Lett.***2009**, *4*, 982–992.
46. Gabrielson, N. P.; Pack, D. W. Acetylation of Polyethyleneimine Enhances Gene Delivery Via Weakened Polymer/ DNA Interactions. *Biomacromolecules***2006**, *7*, 2427–2435.

47. Forrest, M. L.; Meister, G. E.; Koerber, J. T.; Pack, D. W. Partial Acetylation of Polyethylenimine Enhances *in vitro* Gene Delivery. *Pharm Res.* **2004**, *21*, 365–371.
48. Benjaminsen, R. V.; Matthebjerg, M. A.; Henriksen, J. R.; Moghimi, S. M.; Andresen, T. L. The Possible “Proton Sponge” Effect of Polyethylenimine (PEI) Does Not Include Change in Lysosomal pH. *Mol. Ther.* **2013**, *21*, 149–157.
49. Alshamsan, A.; Haddadi, A.; Incani, V.; Samuel, J.; Lavasanifar, A.; Uludag, H. Formulation and Delivery of siRNA by Oleic acid and Stearic Acid Modified Polyethylenimine. *Mol. Pharm.* **2009**, *6*, 121–133.
50. Hu, F. Q.; Chen, W. W.; Zhao, M. D.; Yuan, H.; Du, Y. Z. Effective Antitumor Gene Therapy Delivered by Polyethylenimine-conjugated Stearic Acid-g-Chitosan Oligosaccharide Micelles. *Gene Ther.* **2013**, *20*, 597–606.
51. Kim, W. J.; Cheng, C. W.; Lee, M.; Kim, S. W. Efficient siRNA Delivery Using Water-soluble Lipopolymer for Anti-angiogenic Gene Therapy. *J. Control. Release* **2007**, *118*, 357–363.
52. Guo, S.; Huong, Y.; Wei, T.; Zhang, W.; Wang, W.; Lin, D.; Zhang, X.; Kumar, A.; Du, Q.; Xing, J.; Deng, L.; Liang, Z.; Wang, P. C.; Dong, A.; Liang, X. J. Amphiphilic and Biodegradable Methoxy Polyethylene Glycol-block-(polycaprolactone-graft-poly(2-(dimethylamino)ethyl methacrylate)) as an Effective Gene Carrier. *Biomaterials* **2011**, *32*, 879–889.
53. Liu, Z.; Zhang, Z.; Zhou, C.; Jiao, Y. Hydrophobic Modification of Cationic Polymers for Gene Delivery. *Prog. Polym. Sci.* **2010**, *35*, 1144–1162.

Graphical abstract



A new freeze concentration-based approach was employed that promises to be highly effective for gene therapy applications. This pioneering study shows the effectiveness of this freezing technique at increasing transfection efficiency and is simple, inexpensive, and non-toxic to cells. In addition, a new polyampholyte-based carrier was also developed in order to further optimize the safe and precise delivery of genetic material into target cells. We expect that this enhanced gene transfection strategy using both of these elements will show great potential in a variety of therapeutic applications.

Supporting Information

Freezing Assisted Gene Delivery Combined with Polyampholyte Nanocarriers

*Sana Ahmed,^a Tadashi Nakaji-Hirabayashi,^b Takayoshi Watanabe,^a Takahiro Hohsaka^a and
Kazuaki Matsumura^{a*}*

^aSchool of Materials Science, Japan Advanced Institute of Science and Technology, Nomi,
Ishikawa, Japan

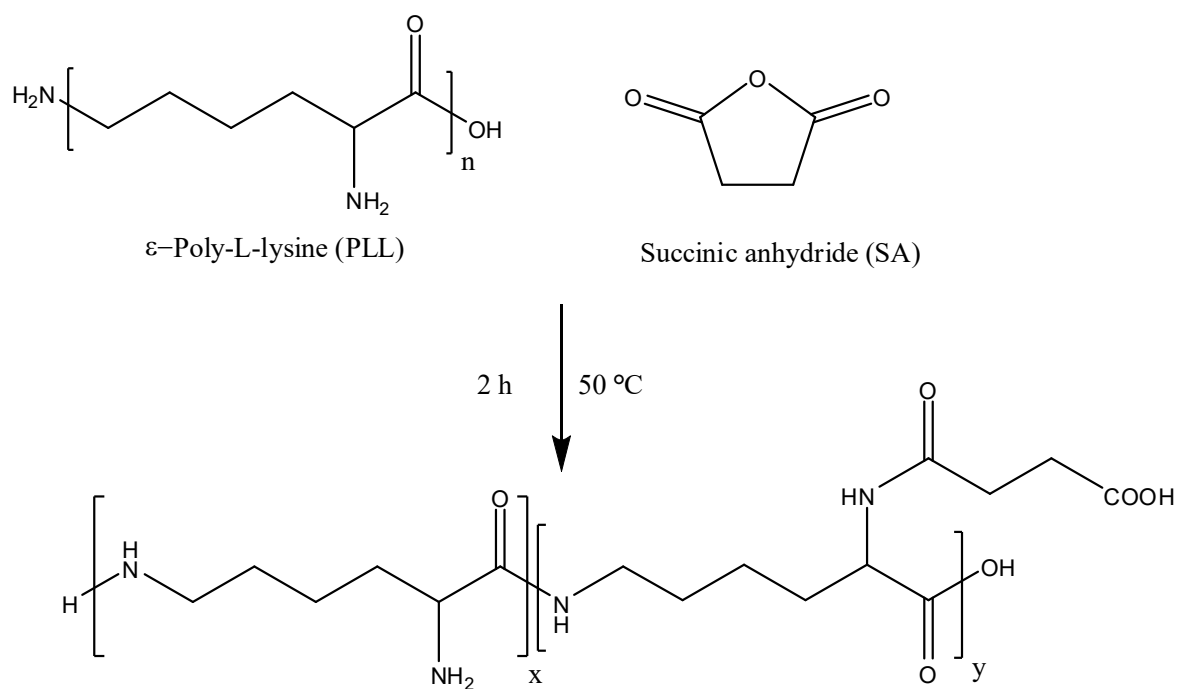
^bGraduate School of Science and Engineering, University of Toyama, 3190 Gofuku, Toyama
930-8555, Japan

*Corresponding Author

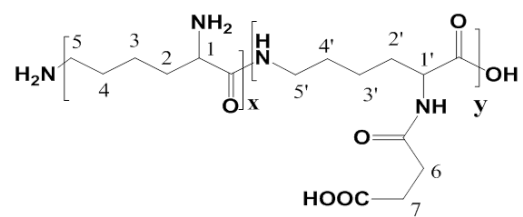
E-mail address: mkazuaki@jaist.ac.jp

Tel: +81-761-51-1680

Fax: +81-761-51-1149



Scheme S1 Schematic representation of the synthesis of the polyampholyte cryoprotectant prepared by succinylation of PLL.



PLL-SA

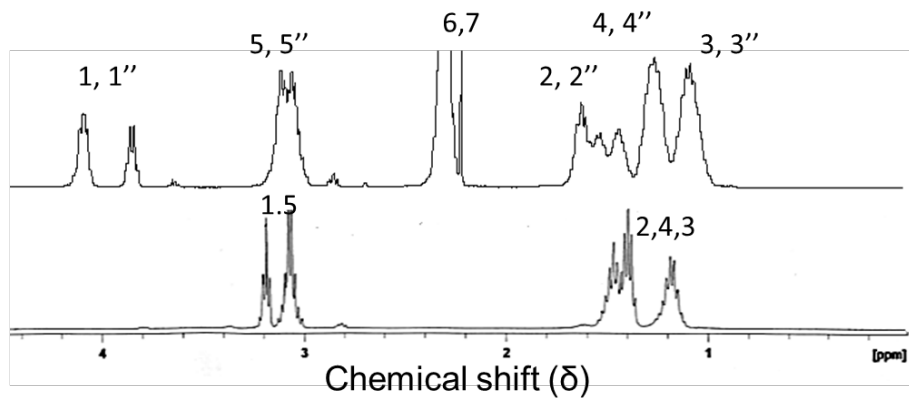


Figure S1. ¹H-NMR of unmodified PLL and PLL-SA.

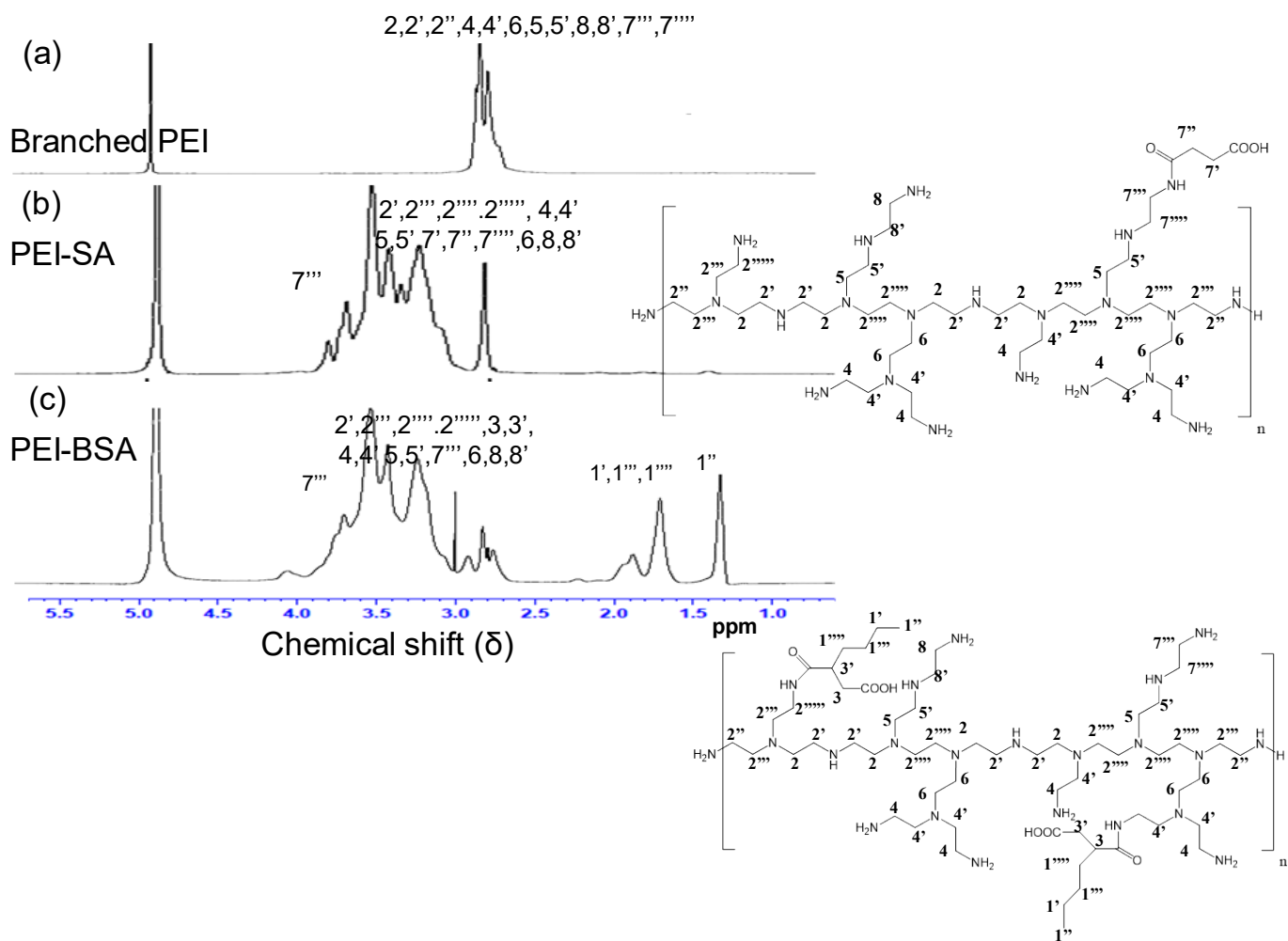


Figure S2. $^1\text{H-NMR}$ of unmodified branched PEI, PEI-SA, and PEI-BSA.

(a)

C1s
C1s Scan A
C1s Scan B

(b)

O1s
O1s Scan A

(c)

N1s Scan A
N1s

(d)

C1s
C1s Scan A
C1s Scan B

(e)

O1s
O1s Scan A

(f)

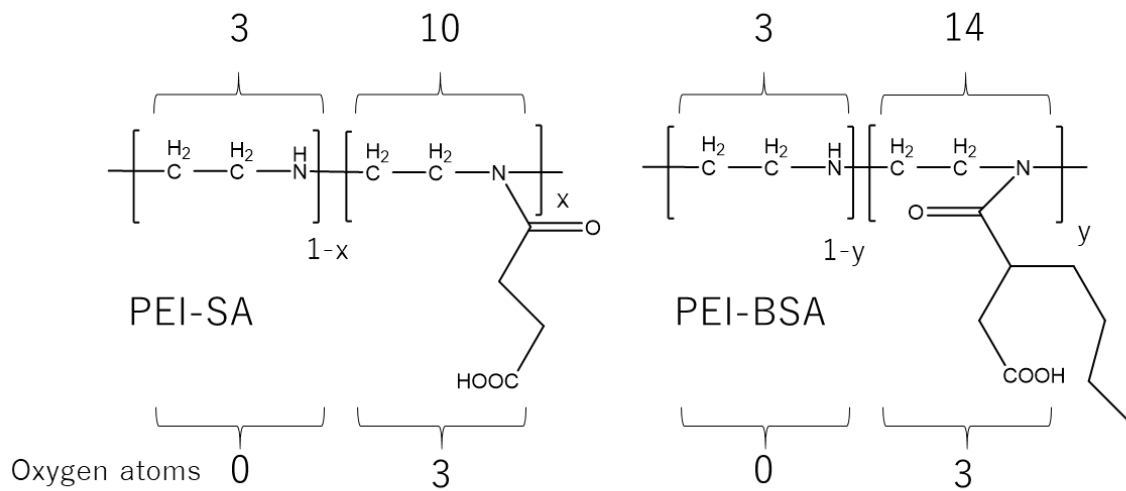
N1s
N1s Scan A

Figure S3. Binding energies of polyampholytes by XPS analysis. PEI-BSA (A) C1s (B) O1s (C) N1s, PEI-SA (D) C1s (E) O1s (F) N1s.

Table S1. Summary of atomic % of each element in PEI-SA and PEI-BSA by XPS analysis

	Atomic % of each element	
	PEI-BSA	PEI-SA
C1s	48.27	52.76
C1sA	20.41	14.59
C1sB	4.52	3.16
Total C	73.22	70.52
N1s	9.37	10.47
N1sA	10.49	11.30
Total N	19.86	21.78
O1s	4.78	5.54
O1sA	2.12	2.14
Total O	6.90	7.69

Total atoms present except hydrogen



X_o = Oxygen atomic % in PEI-SA

Y_o = Oxygen atomic % in PEI-BSA

$$\frac{3 * \frac{x}{100}}{3 * \left(1 - \frac{x}{100}\right) + 10 * \frac{x}{100}} = \frac{X_o}{100}$$

$$\frac{3 * \frac{y}{100}}{3 * \left(1 - \frac{y}{100}\right) + 14 * \frac{y}{100}} = \frac{Y_o}{100}$$

Here, we can calculate the degree of substitution: $x = 9.38$ and $y = 9.35$ in Table 1.

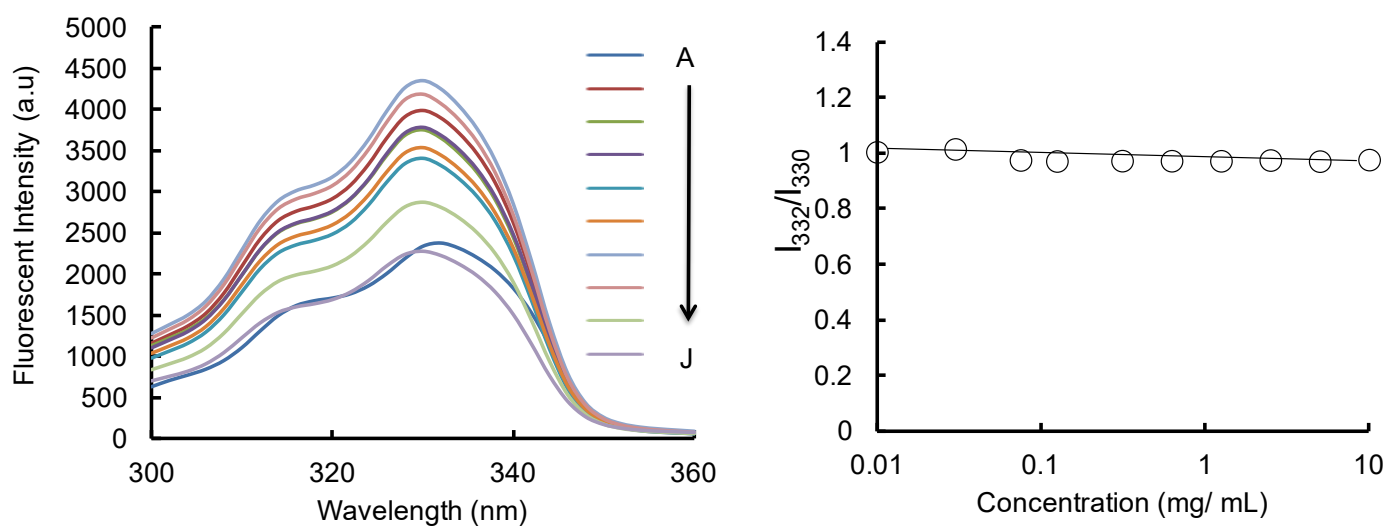


Figure S4. CACs of branched PEI. (a) Pyrene excitation spectra (A-J) of PEI-BSA solutions at different polyampholyte concentrations, 10, 5, 2.5, 1.25, 0.625, 0.312, 0.125, 0.075, 0.032 and 0.01 mg/mL, respectively. (b) The ratio of I_{332}/I_{330} against polymer concentration.

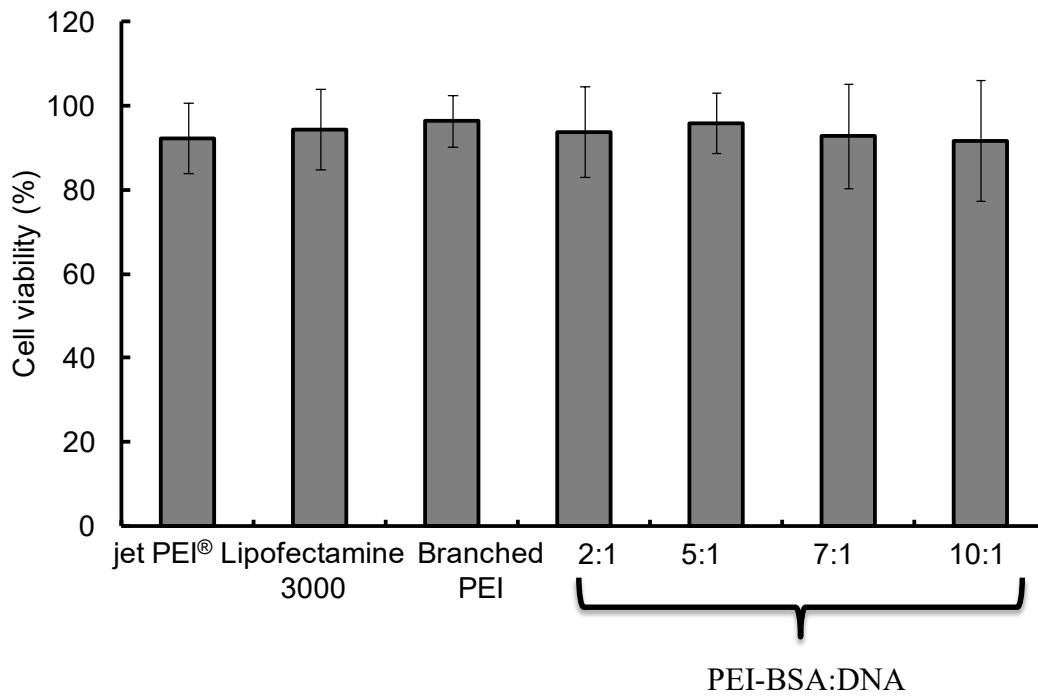
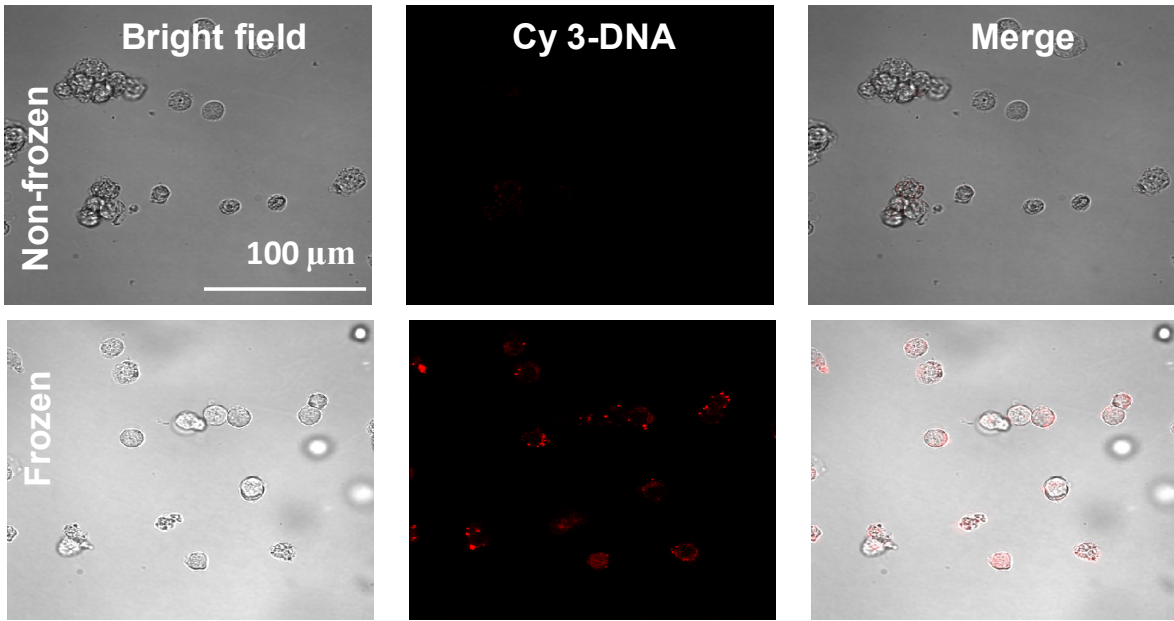
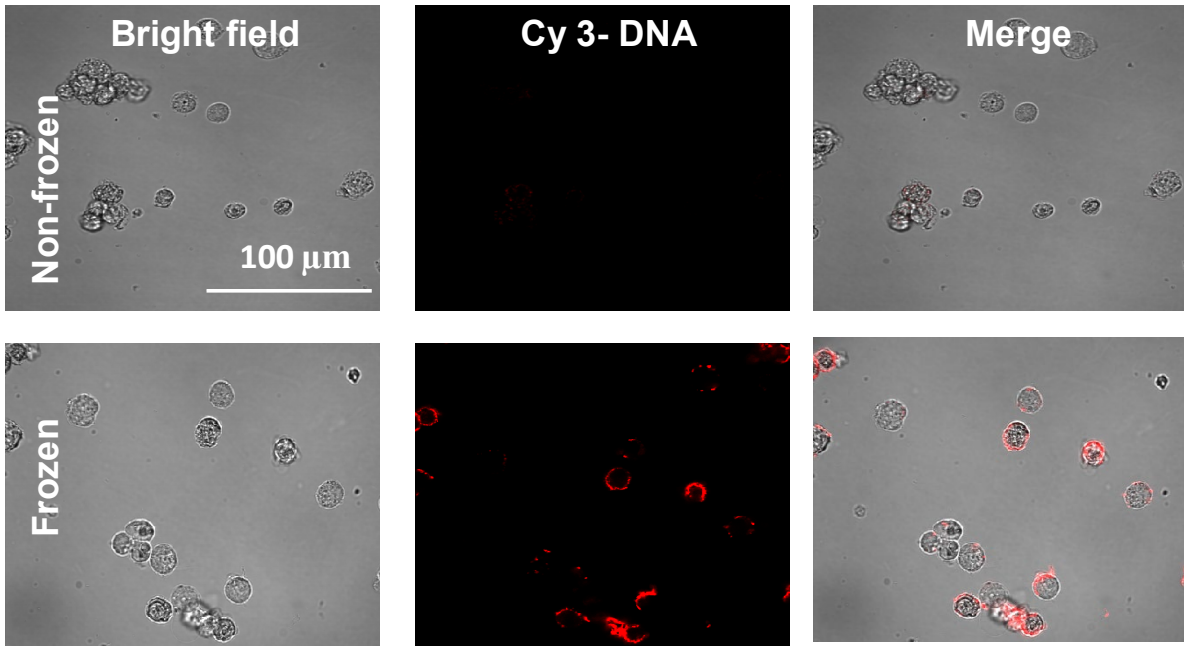


Figure S5. HEK-293T cell viability after being frozen at -80°C for one day with either the commercially available transfection carriers jetPEI[®] and Lipofectamine3000, branched PEI with pDNA ($1\mu\text{g}$), or containing the indicated ratios of PEI-BSA:pDNA (w/w). All cells were frozen in the presence of the cryoprotective solution 10% PLL-SA. Data are expressed as mean \pm SD

(A) With jet PEI®



(B) With Polyampholyte Nanoparticles PEI-BSA



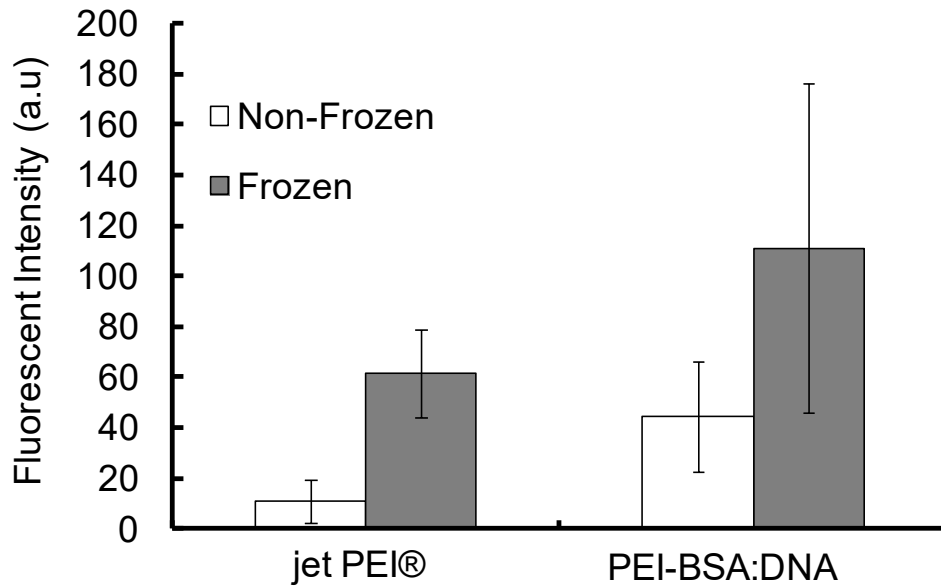
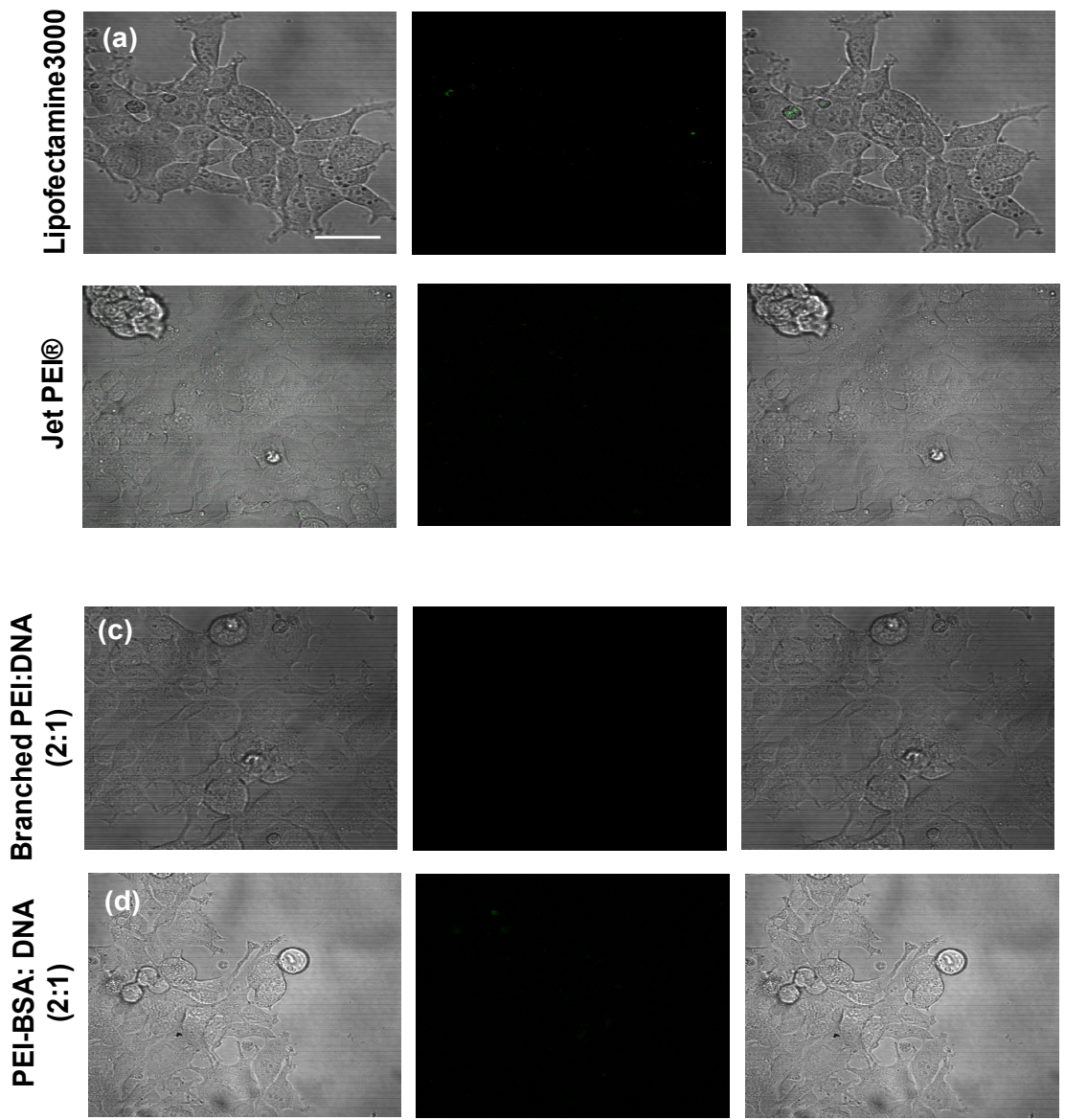


Figure S6. Confocal images of HEK-293T cells before and after freezing with Cy3-labeled pDNA in the presence of 10% PLL-SA as a cryoprotectant. Cy 3 fluorescence is shown in red (A) jetPEI®:DNA (2:1, w/w) (B) PEI-BSA:DNA (2:1, w/w). Scale bars: 100 μ m. (C) Mean fluorescence intensity of Cy3-labeled pDNA adsorbed onto HEK293-T cells before and after being frozen, using either jetPEI® or PEI-BSA as carrier, as determined by confocal microscopy. Data are expressed as mean \pm SD



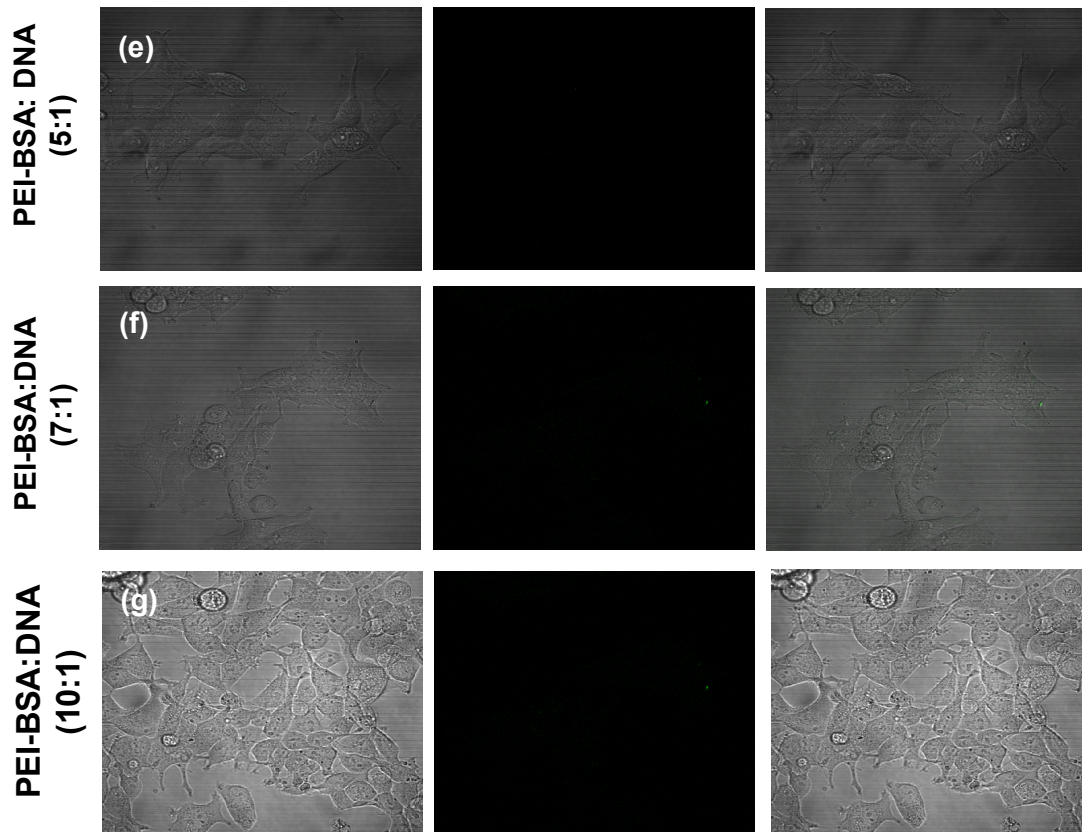


Figure S7. Confocal microscopy images showing GFP expression. *In vitro* transfection of DNA complexes in HEK 293 T cells were incubated in the presence of 10% PLL-SA as a cryoprotectant without freezing was incubated for 10 h. A) Each commercially available transfection reagents was incubated with plasmid DNA (1 μ g) (a) Lipofectamine 3000 (b) jetPEI[®] (c) Branched PEI:pDNA (2:1,w/w), PEI-BSA:DNA (d) 2:1 (e) 5:1 (f) 7:1 (g) 10:1, w/w).